Networks and Spatial Economics (2021) 21:85–122
https://doi.org/10.1007/s11067-020-09508-3

# Delay, Throughput and Emission Tradeoffs in Airport Runway Scheduling with Uncertainty Considerations

Jianan Yin[1,2] · Yuanyuan Ma[3] · Yuxin Hu[3] · Ke Han[4] · Suwan Yin[2] · Hua Xie[1]

Accepted: 1 September 2020 / Published online: 21 November 2020


## Abstract

Runway systems are among the most stringent bottlenecks at global hub airports, which have been identified as a major source of airport inefficiency. Runway system inefficiencies are manifested in multiple dimensions such as delay, throughput reduction and excessive emission, whose tradeoffs are investigated in this paper as part of an airport runway scheduling problem in the presence of uncertainty. We formulate a multi-objective optimization model aiming to minimize flight delays, maximize airport throughput, and minimize aircraft emissions, subject to a variety of constraints such as minimum separation, time window, runway occupancy and flight turnaround. The computational performance is enhanced with an efficient multi-objective evolutionary algorithm, with two mechanisms of adaptive and controllable time-coding and objective-guided individual selection. The proposed method is flexible in adjusting conservatism when it comes to optimization with uncertainty, and offers a set of Pareto optimal solutions for different stakeholders without using scalarization of different objectives. A real-world case study is carried out for one of the world's buiest airports, Shanghai Pudong, under the case of 2 runways, 2 operation types, 12 uncertain conditions and 4 tradeoff scenarios. The computational results show that the proposed optimized method has overall advantages in improving the runway scheduling performance over some meta-heuristics and the First Come First Served strategy. The tradeoff analysis reveals that the minimum delay schedule is preferable for balancing delay, throughtput and emission. The findings provide managerial insights regarding traffic management measures for different stakeholders at high-density airports.

**Keywords** Air traffic management · Runway scheduling · Performance tradeoff · Uncertainty · Multi-objective optimization · Evolutionary algorithm

✉ Jianan Yin
j.yin@nuaa.edu.cn

Extended author information available on the last page of the article

**Nomenclature**

| | |
|---|---|
| ARSP | Airport Runway Scheduling Problem |
| ATM | Air Traffic Management |
| EMOE | Efficient Multi-Objective Evolutionary |
| ACTC | Adaptive and Controllable Time-Coding |
| OGIS | Objective-Guided Individual Selection |
| TMA | Terminal Manoeuvring Area |
| FCFS | First Come First Served |

## 1 Introduction

Airports are the key nodes of an air transport network. Their operational efficiency is, therefore, crucial to the system-wide performance of national airspace system. It has been reported that the bottleneck of air traffic operations has been shifted from en-route airspace to the airports (Smeltink et al. 2003; Yin et al. 2019), partly due to the consistent improvements made in the en-route air traffic management. At many hub airports, the insufficient capacity cannot accommodate high traffic demands (Lozano and Gutiérrez 2011). The runway system, in particular the multi-runway system, has been identified as the major source of airport inefficiency (Sölveling and Clarke 2014). When the runway system is operating under imbalanced demand and supply (capacity), the resulting excessive congestions, long flight queues, and the increased level of environmental impacts are commonly observed, causing inconvenience and costs to passengers and airlines (Sölveling et al. 2011).

Major hub airports have taken measures such as infrastructure investments and better resource utilization in order to enhance the airport operational performance. Although airport capacity can be increased through infrastructure investments, such as constructing a new runway or expanding an existing one, such measures receive secondary priority given their excessive costs and long construction period. Actually, the planning, design and construction of airport infrastructure is notoriously lengthy and create challenges for airport capacity planners. A more practical and effective solution to better balance demand and capacity is to improve the planning and execution of resource utilization to achieve higher efficiency and maximized social welfare within the given capacity limitation. Therefore, for an existing airport system, making use of the limited capacity and scheduling aircraft landings and take-offs are important to enhance airport performance and flight efficiency without increasing infrastructure investment.

### 1.1 Problem Description

The Airport Runway Scheduling Problem (ARSP) seeks to determine the sequences and times of the arrivals, departures or a combination to optimize some specific objectives, subject to a variety of operational constraints (Bennell et al. 2011). ARSP, or scheduling in general, tends to be a highly complex mathematical programming problem, with numerous operational constraints in a real-time decision environment. Figure 1 shows a general description of aircraft operations in an airport system. From the perspective of resource modeling, ARSP consists of spatial scheduling and

temporal scheduling decisions (Yin et al. 2015). The spatial scheduling process determines the sequence in which aircraft land or take-off, as well as the assigned runways under the condition of multi-runway operations. The aim of temporal scheduling is to give an assigned landing or take-off time to each aircraft in a specific runway sequence.

Efficient runway scheduling can reduce the number of long separation times thereby providing new slots of runway usage for the landings and take-offs. The key constraints in runway scheduling are safety requirements, for example, the minimum separations between landings, between take-offs, or between landing and take-off, runway occupancy separations, and flight connection separations. Additionally, many current studies ignore the process of aircraft turnaround operations, or also referred to aircraft ground handling. In this paper, we consider the minimum turnaround separations, which is defined as the time required to unload the aircraft after its arrival at the gate and to prepare it for departure again. Besides the above separation issues, there are also some issues which other stakeholders are interested in (Lee and Balakrishnan 2008; Bennell et al. 2017). Air transport encompasses a number of stakeholders including air navigation service providers, airports, airlines, government and passengers, each comes with their own priority and decision-making target. The first important target is reducing flight delays, which is a common concern for airports, airlines and passengers. More delays lead to excessive costs such as the airborne and ground holding costs, and may have a detrimental impact on the rate of flight punctuality resulting in a reduced passenger satisfaction. Airport throughput is also important to increase the performance of airports and air navigation service providers. The governments and some organisations have goals of reducing aircraft emissions to maintain the sustainability of social and economic development. In a dynamic environment with multiple factors of weather conditions, traffic management initiatives, human factors and other circumstances, the input parameters are inevitably deviated from the initial scheduled time. Hence, the runway scheduling in the presence of uncertainty, and the tradeoffs among multiple performance indicators are the main concerns of this paper.

### 1.2 Literature Review

The performance of runway scheduling in airport systems, especially in major airports with multiple runways, is crucial to the efficiency of arrivals and departures. The dynamic and timely nature of aircraft movements necessitates the development of ARSP models and algorithms that are computationally efficient, and therefore

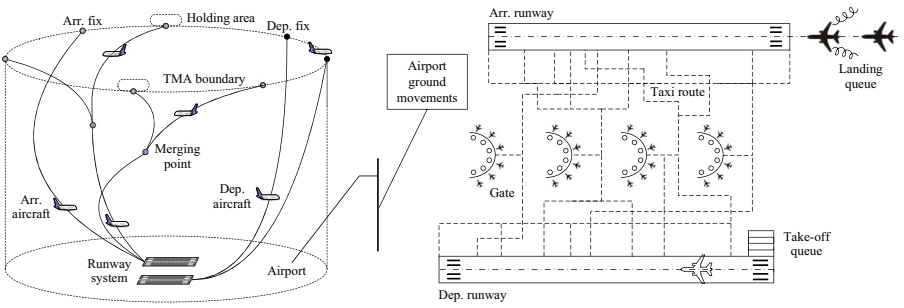


**Fig. 1** General description of aircraft operations in an airport system

amenable to new information and uncertain circumstances. Generally, ARSP can be formulated as similar problems in other research fields (D'Ariano et al. 2015). For example, in job shop scheduling models, the jobs correspond to landing or take-off operations, and the machines represent the runway system. The sequence-dependent processing times correspond to the minimum separations between each pair of aircraft (Brentnall 2006). For the models of travelling salesman problem, the intercity distances are replaced with minimum separations, and the restriction of finishing the tour where it was started is removed (Luenberger 1988). In quadratic assignment models, the landing or take-off operations represent the facilities, and the runways represent the locations (Martyna 2012). Also, the ARSP can be viewed as a type of dynamic traffic assignment problem (Han et al. 2019) in which all the aircraft in an airport system engage in a competitive environment with arrival time, departure time and route choices. Ng et al. (2018) and Bennell et al. (2011) have present a wide review of the current research about ARSP. Although many advances have been made in the existing studies, Bennell et al. (2017) present that most of the models usually focus on a single performance metric and do not address the concerns from multiple stakeholders in a practical decision-making environment, and many of the algorithms have not been tested using real data. ARSP is still among the most challenging area in the air transport sector.

Samà et al. (2017a) present a number of related literature classifications based on different modeling perspectives, e.g., single-airport / multi-airport scheduling (from the perspective of traffic control), static and dynamic scheduling (from the perspective of information type). Based on the type of aircraft movements, ARSP includes landing, take-off and integrated scheduling (Ma et al. 2015, 2017; Sölveling and Clarke 2014; Atkin et al. 2008), corresponding to different runway configurations and scheduling environment. The landing and take-off scheduling problems are generally modeled and solved separately in most of existing studies, and the integrated scheduling has received great attention in the past few years. In real-world context, a flight operates under a variety of factors such as weather conditions, pilot and controller behaviors and surrounding air traffic flow, which may create some uncertainties in ARSP. For example, the input information of initial arrival and departure times. The existing ARSP models can be grouped as deterministic and stochastic / robust. In the deterministic ARSP, the models assume that the input parameters of runway time (e.g., earliest landing time, target take-off time) are known (Balakrishnan and Chandran 2010). Compared with the deterministic case, only a few of the existing literature about ARSP focus on the stochastic / robust cases. Stochastic / robust ARSP in the literature primarily focus on uncertain characteristics of input parameters (Ng et al. 2020; Ng et al. 2017a; Ng et al. 2017b; Xue and Zelinski 2015; Samà et al. 2013; Sölveling 2012). In this paper, we focus on the single-airport landing and take-off scheduling in a static environment with uncertain air traffic demand.

Most of the existing studies focus on ARSP in a single runway system (Avella et al. 2017; Gupta et al. 2011; Atkin et al. 2008), or single-objective optimization in a multi-runway system (Ng et al. 2017a; Lieder and Stolletz 2016; Balakrishnan and Chandran 2006). The optimization objectives are mainly related to the performance of Air Traffic Management (ATM), airport, airlines, government and passengers (Yin et al. 2015; Yin et al. 2014a; Yin et al. 2014b; Kim et al. 2010; Balakrishnan and Chandran 2010). The related objectives of ARSP are as follows.

- **ATM objectives**. Maximize: runway throughput, flight fairness; Minimize: flight delays, scheduling makespan; controllers' workload, surface conflicts.
- **Airport objectives**. Maximize: capacity ultilization, rate of flight punctuality; Minimize: change rate of gate allocation due to flight delays.
- **Airlines objectives**. Maximize: airlines preferences, punctuality according to the published timetables; Minimize: aircraft taxiing time, change rate of gate allocation due to flight delays.
- **Government objectives**. Minimize: environmental impacts, such as the emissions and noise.
- **Passenger objectives**. Minimize: waiting time before departure.

Ideally, in order to meet the aims of various stakeholders in air transport industry, the above list of ARSP objectives should be taken into account at the same time. However, these objectives from different perspectives may conflict with each other. For example, under a fixed amount of time advance (i.e., the negative delays), the decrease in operational cost may be achieved at the expense of an increase in average delay. The optimal schedule to maximize the airport throughput or minimize the scheduling makespan may not an option to minimize the flight delays (Lee and Balakrishnan 2008). Although a weighted sum of objective function is often used to convert the multi-objective optimization to single-objective optimization in the existing ARSP optimization, there is a shortcoming that these weights are artificially set by researchers (Heidt et al. 2016; Atkin et al. 2008; Atkin et al. 2007) and there is no flexibility of getting different solutions to meet multiple needs of the above stakeholders.

The ARSP has been proved as a typical NP-hard problem (Ng et al. 2018; Samà et al. 2017b; Bennell et al. 2011), which suffers from curse of dimensionality for problems in real-time applications (Beasley et al. 2001; Mesgarpour et al. 2010). Generally, the optimal solution cannot be gotten using models that include all operational constraints, especially for a large planning horizon. A variety of algorithms have been proposed in the existing ARSP researches, which can be mainly divided into two categories: exact algorithms (Ng et al. 2017b; Montoya et al. 2014; Rathinam et al. 2009) and approximation algorithms (Heidt et al. 2014; Nikoleris et al. 2010; Bayen et al. 2004). Although the unique global optimal solution has a theoretical significance, sometimes it cannot meet different needs from all the stakeholders in air transport industry, especially for the tradeoffs among multiple performance indicators. As typical approximation algorithms, heuristic algorithms (Samà et al. 2018; Furini et al. 2015; Vadlamani and Hosseini 2014) and meta-heuristic algorithms (Ma et al. 2017; Sabar and Kendall 2015; Atkin et al. 2007) are generally adopted in practice to solve the NP-hard problem and compute good quality solutions in a short computation time. The majority of the research on ARSP has focused on developing meta-heuristic algorithms, especially for the genetic algorithm (Ma et al. 2015, 2017; Yin et al. 2014b; Hansen 2004; Beasley et al. 2001).

Although some works are related to the stochastic and robust ARSP, the overview shows that most of the studies optimize the ARSP under a single objective or a weighted sum of objective functions, while very few studies focus on the tradeoffs among different performance metrics without using weight coefficients. Regarding the tradeoffs, we think that air traffic controllers should be informed of a set of tradeoff solutions to satisfy the decision needs from different stakeholders in practice and of the

potential impact of each solution in terms of multiple performance metrics. To this end, this paper addresses the evaluation of a number of ARSP performance metrics under different minimum runway schedules, and then conduct analyses of tradeoffs among these metrics without using a traditionally integrated objective function.

### 1.3 Contribution of the Research

This paper proposes an optimization and tradeoff framework for ARSP under uncertain conditions, and makes contributions in the following areas:

- A novel ARSP model is developed to make flexible and non-weighted tradeoffs among multiple performance indicators, characterized by simultaneous consideration of (i) a multi-runway system (two parallel runways), (ii) an integrated scheduling (landings and take-offs), (iii) operational uncertainties (two uncertain parameters) and (iv) multi-objective (delays, throughput and emissions) tradeoffs. To the best of our knowledge, few studies have given consideration to the complexity expressed by (i)-(iv) as our paper in ARSP.
- The proposed Efficient Multi-Objective Evolutionary (EMOE) algorithm is adjustable with flexibility of choosing Pareto optimal solutions and can be effectively applied to make tradeoffs among different optimization objectives. Two mechanisms are designed to enhance EMOE performance: The Adaptive and Controllable Time-Coding (ACTC) mechanism integrates the acceptable maximum delay, turnaround time and Hamming distance to improve the initialisation of evolution process. The Objective-Guided Individual Selection (OGIS) mechanism is featured by four parts: preferred level identification, single-level assessment, cross-level assessment, and inducing evolution strategy.
- We provide a comparative ARSP study under different uncertain conditions and single / multiple minimum schedules on practical-size instances from Shanghai Pudong International Airport (PVG). Our method outperforms some metaheuristics and First Come First Served (FCFS) in terms of minimizing delays and emissions and maximizing throughput. The developed framework is flexible and can be applied for a better understanding of how the different ARSP performance indicators interact with each other in a multi-user competitive environment with conflicts of interest. Our research work is complementary to the single-objective and weighted multi-objective ARSP optimization done in the existing literature.

### 1.4 Organisation of the Paper

The organisation of this paper is summarized as follows. After the introduction of ARSP and research summary in Section 1, we formulate a new runway scheduling model with uncertainty considerations in Section 2, for the tradeoffs among delays, throughput and emissions. Section 3 presents our EMOE algorithm with ACTC and OGIS mechanisms. Section 4 and Section 5 report the computational performance, numerical results and tradeoff analyses for PVG. Finally, the discussions and conclusions are raised in Section 6.

## 2 Mathematical Formulation

In this paper, a multi-objective Airport Runway Scheduling Problem (ARSP) with uncertainties about arrival and departure fluctuations is considered, aiming to enhance the performance of runway scheduling with the objectives of flight delays, airport throughput and aircraft emissions. Note that the runway configuration of segregated parallel operations is widespread in China and plays an important role in the Chinese airport operational practice. Many Chinese airports have resorted to segregated parallel operations as a trial and key runway mode. For instance, *PEK*, *CAN*, *PVG*, *SHA*, *SZX*, *HGH*, *NKG* and *TSN* airports are, or were, characterized by segregated parallel operations as one of the most key modes at the initial stage of multi-runway operations. In this paper, we select a common runway configuration of segregated parallel operations (34|35R) in Shanghai Pudong airport with three-runway layout for analysis. The assumptions for the ARSP are outlined below.

(a). The runway configuration is fixed for segregated parallel operations and it will not be changed during the ARSP process;
(b). For each combination of runway and fix in the Terminal Manoeuvring Area (TMA), there will be a pre-determined transition paths between them;
(c). There are no serious disturbances in the planning horizon, and then no aircraft rerouting and retiming once the optimized schedule is formulated.

### 2.1 Notations

Let $F$ be the set of all flights within the planning horizon. $A$, $D \subseteq F$ correspond to the arrivals and departures, respectively, sorted in ascending order of initial scheduled time $E_i^a$ (for arrival) and $E_k^d$ (for departure) of runway usage. That is to say, if $i, j \in A$ then $i > j$ implies $E_i^a \geq E_j^a$. The sets, parameters and variables of the ARSP formulation are shown in Table 1.

According to the interaction relationship between arrivals and departures under different runway configurations, a runway assignment variable may be needed in ARSP models (Lieder and Stolletz 2016; Ng et al. 2017a). The runway assignment variable is introduced to specify which arrival (departure) runway is used for landing (take-off) operations, if there are more than one arrival (departure) runways. In this paper, the runway configuration is set to the segregated parallel operations, which are simultaneous operations on a two-runway system in which one runway is used exclusively for landings and the other is used exclusively for take-offs. Hence, we focus on the assignment variables of landing time and take-off time in our proposed ARSP model.

### 2.2 Objectives

We seek to optimize the ARSP performance and make tradeoffs among different metrics of flight delays, airport throughput (i.e., scheduling makespan) and aircraft emissions. The objective functions for our optimization problem can be seen in Eqs. (1)–(5).

**Table 1** Sets, parameters and variables of the ARSP formulation

| | |
|---|---|
| **Sets** | |
| $F$ | The set of all the flights within the planning horizon |
| $A$ | The set of arrivals sorted in ascending order of $E_i^a$, $A \subseteq F$ |
| $D$ | The set of departures sorted in ascending order of $E_k^d$, $D \subseteq F$ |
| $\Phi$ | The set of pairs of connected flights corresponding to turnaround processes |
| **Parameters** | |
| $E_i^a, E_k^d$ | The initial landing (take-off) time of arrival (departure) aircraft $i$ ($k$) |
| $\eta$, $\Lambda$ | Uncertainty coefficients of probability and interval |
| $s$ | The mode of landing and take-off cycle. $s = 1, 2, 3$ denote arrival (descent, approach), taxiing (taxi-in, taxi-out) and departure (take-off, climb), respectively. |
| $f_i^s$ | The fuel flow rate of aircraft $i$ in mode $s$, considering the number of engines |
| $m$ | The type of emission. $m = 1, 2, 3$ denote HC, CO and NOx pollutants, respectively, based on ICAO's Emissions Databank |
| $e_i^{ms}$ | The emission index of pollutant $m$ from aircraft $i$ in period $s$ |
| $\mathcal{L}_i^a, \mathcal{L}_k^d$ | The amount of emissions HC, CO and $NO_x$ from the engine of arrival (departure) aircraft $i$ ($k$) |
| $P_i^a, P_k^d$ | The operation time of arrival (departure) aircraft $i$ ($k$) in the TMA |
| $Q_i^a, Q_k^d$ | The taxi-in (taxi-out) time of arrival (departure) aircraft $i$ ($k$) at airport ground area |
| $\lambda^+$, $\lambda^-$ | The acceptable maximum delay (gray delay, corresponding to the negative delay) of each aircraft |
| $M$ | A large enough positive integer, for the constraint analysis |
| $s_{ij}^a, s_{kl}^d$ | The minimum separation of arrival (departure) aircraft $i$ ($k$) and $j$ ($l$) |
| $d_{ij}$ | The spatial (e.g., radar) separation between aircraft $i$ and $j$ |
| $v_i$ | The speed of aircraft $i$ |
| $\tau_j^a, \tau_l^d$ | The runway occupancy time of arrival (departure) aircraft $j$ ($l$) |
| $\xi_{ik}$ | 1 if departure aircraft $k$ and arrival aircraft $i$ are a pair of connected flights, 0 otherwise |
| $\chi_{ik}$ | The minimum connection time between the take-off time of departure aircraft $k$ and landing time of arrival aircraft $i$ |
| **Variables** | |
| $T_i^a, T_k^d$ | The assigned landing (take-off) time of aircraft $i$ ($k$) |
| $\varphi_{ij}^a, \varphi_{kl}^d$ | 1 if arrival (departure) aircraft $i$ ($k$) lands on (takes off from) the runway system after $j$ ($l$), 0 otherwise |

(1) **Minimize flight delays.** The model minimizes the total waiting time spent by all arrivals and departures beyond the initial scheduled time.

$$\min \sum_{i \in A} \left| T_i^a - E_i^a \right| + \sum_{k \in D} \left| T_k^d - E_k^d \right| \tag{1}$$

The flight delay of each arrival (departure) aircraft is defined as the difference between the assigned landing (take-off) time and the initial landing (take-off) time. Note that in order to ensure flight punctuality as much as possible, the negative delays in the presence of time advance of arrival and departure are also counted as delays in terms of absolute value.

(2) **Minimize scheduling makespan.** The model minimizes the completion time of the aircraft scheduling sequence in airport runway system.

$$\min\left\{\max\left(T^a_{|A|}, T^d_{|D|}\right) - \min\left(T^a_1, T^d_1\right)\right\} \tag{2}$$

where $|A|$ and $|D|$ are respectively the quantity of arrivals and departures.

The makespan is defined as the difference between the last and first runway time in the aircraft scheduling sequence. For a fixed set of arrivals and departures, if all the runways are considered as a whole system, we can make an approximately equivalent transformation between the maximization of airport throughput and the minimization of scheduling makespan. In the real practice, the transformation is desirable from the perspective of ATM.

(3) **Minimize aircraft emissions.** The model minimizes the total amount of emissions HC, CO and $NO_x$ from the engine of aircraft.

$$\min \sum_{i\in A} \mathcal{L}^a_i + \sum_{k\in D} \mathcal{L}^d_k \tag{3}$$

$$\mathcal{L}^a_i = \sum_{m\in P}\left(P^a_i f^1_i e^{m,1}_i + Q^a_i f^2_i e^{m,2}_i\right) \tag{4}$$

$$\mathcal{L}^d_k = \sum_{m\in P}\left(Q^d_k f^2_k e^{m,2}_k + P^d_k f^3_k e^{m,3}_k\right) \tag{5}$$

Since each flight mode has different engine power settings and vertical profile such as altitude and speed, the associated emissions are calculated separately. In this paper, our calculation of aircraft emissions is mainly based on the ICAO reference method, which uses the operation time, the fuel flow rate and the emission index to calculate the aircraft emissions for different engine conditions. Note that the input of fuel flow rate considers the number of aeronautical engine.

### 2.3 Constraints

A feasible scheduled sequence must meet the constraints of minimum separation, time window, runway occupancy and flight turnaround. The constraints for our optimization problem can be seen in Eqs. (6)–(13).

(1) **Minimum separation constraints.** For the landings and take-offs considered here, the minimum separation $s_{ij}^a$ and $s_{ij}^d$ are required to hold, which defines the minimum separation (e.g., wake-vortex separation, and miles-in-trail restriction) between succeeding and preceding aircraft.

$$T_i^a - T_j^a \geq s_{ij}^a - M\left(1-\varphi_{ij}^a\right), \forall i, j \in A \tag{6}$$

$$T_k^d - T_l^d \geq s_{kl}^d - M\left(1-\varphi_{kl}^d\right), \forall k, l \in D \tag{7}$$

Without loss of generality, we take Eq. (6) for an example to present the computation of separation. Let $i$ and $j$ are the succeeding and preceding aircraft, respectively. $v_i$ and $v_j$ are the speed of $i$ and $j$, which is set based on the weight class of aircraft (e.g., heavy, medium, light). Figure 2 illustrates the projection of spatial-temporal separation for a landing sequence.

If $v_j \leq v_i$, then the separation $d_{ij}$ between $i$ and $j$ will reach the minimum at the runway entrance; otherwise, it will reach to the minimum at the entrance of common

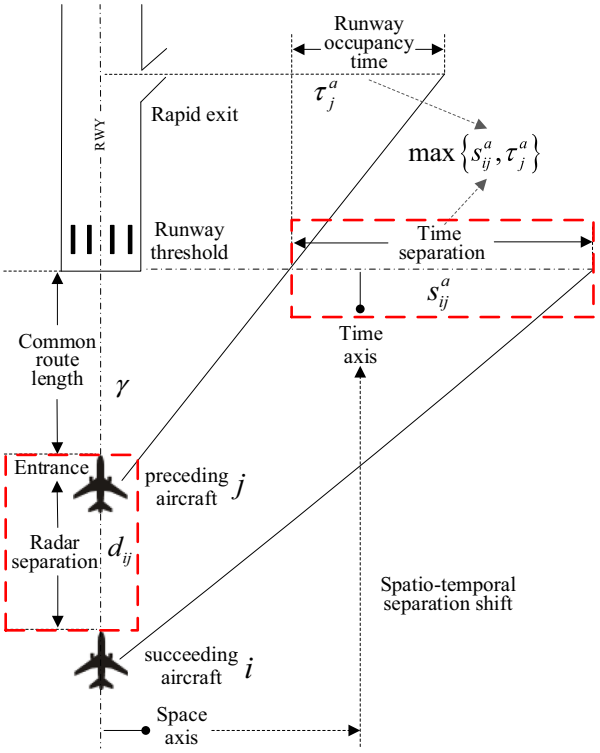


**Fig. 2** The projection of spatial-temporal separation for a landing sequence

route with a length of $\gamma$. Then we can project the spatial separation $d_{ij}$ to the temporal separation $s_{ij}^a$.

$$s_{ij}^a = \begin{cases} \dfrac{d_{ij}}{v_i} & , v_j \le v_i \\ \dfrac{d_{ij}}{v_i} + \gamma\left(\dfrac{1}{v_i} - \dfrac{1}{v_j}\right), & v_i > v_k \end{cases} \tag{8}$$

(2) **Time window constraints.** Let each aircraft be subject to a time window that is defined by its initial scheduled time and acceptable maximum delay. Then the assigned landing time and take-off time must be within the window $\left[E_i^a - \lambda^-, E_i^a + \lambda^+\right]$ and $\left[E_k^d - \lambda^-, E_k^d + \lambda^+\right]$, respectively.

$$T_i^a - E_i^a \in [-\lambda^-, \lambda^+], \forall i \in A \tag{9}$$

$$T_k^d - E_k^d \in [-\lambda^-, \lambda^+], \forall k \in D \tag{10}$$

If the aircraft is speeded up (prepared earlier) before its arrival (departure), the actual runway time will be earlier than the estimated runway time. Here we define the negative delay as "gray delay", meaning that the assigned time ($T_i^a$ or $T_k^d$) is ahead of the initial time ($E_i^a$ or $E_k^d$). Actually, the gray delay is a common phenomenon in air transport industry, especially in China, which is the world's second largest aviation market. In our model, we set the acceptable maximum delay $\lambda^+$ and gray delay $\lambda^-$ based on the airport investigation, turnaround time statistics and airline preferences.

(3) **Runway occupancy constraints.** For the landings or take-offs in the same runway, the runway occupancy time is also required to hold, which is used to ensure that each runway cannot simultaneously used by two or more aircraft at the same time.

$$T_i^a - T_j^a \ge \tau_j^a - M\left(1 - \varphi_{ij}^a\right), \forall i, j \in A \tag{11}$$

$$T_k^d - T_l^d \ge \tau_l^d - M\left(1 - \varphi_{kl}^d\right), \forall k, l \in D \tag{12}$$

For the arrival sequence, if j does not exit the runway when $i$ reaches the runway threshold, the separation $s_{ij}^a$ should be increased by considering $\tau_j^a$. Therefore, the minimum separation between $i$ and $j$ should be the maximum between $s_{ij}^a$ and $\tau_j^a$. Generally, for the heavy and medium weight class of aircraft, the $\tau_j^a$ is smaller than the $s_{ij}^a$. In our case study, there is no small aircraft in the planning horizon and then the Eqs. (11) and (12) hold if Eqs. (6) and (7) hold.

(4) **Flight turnaround constraint.** Let departure aircraft $k$ and arrival aircraft $i$ be a pair of connected flights, that is to say arrival aircraft $i$ will be pushed back from the gate by the identification of departure aircraft $k$ after the turnaround process of $i$. Then the difference between the assigned take-off time of departure aircraft $k$ and the assigned landing time of arrival aircraft $i$ must be larger than the minimum connection coefficient $\chi_{ik}$.

$$T_k^d - T_i^a \geq \chi_{ik} - M(1-\xi_{ik}), \forall k \in D, \forall i \in A, (i,k) \in \Phi \tag{13}$$

By analyzing the whole process of aircraft ground movements, we suggest setting the value of $\chi_{ik}$ to the sum of minimum turnaround time, taxi-in time and taxi-out time. Actually, by integrating the runway times and taxiing times, Eq. (13) ensures the minimum difference between gate-in and gate-out time, i.e., there is enough time to unload aircraft $i$ after its arrival at the gate and to prepare it for the following departure aircraft $k$ again.

### 2.4 Uncertainty Setting

ATM measures derived based on deterministic and stationary information face challenges posed by operational uncertainties (Malik et al. 2016; Bosson et al. 2015), which may be caused by mutual disturbance between different airspace users, aircraft boarding process reliability, inaccurate weather forecast, and human factors. For example, the general and military aviation will impact the commercial aviation and impose deviations from the initial schedule. The behaviors of passenger, pilot and shuttle driver will impact the boarding process or flight efficiency. Especially, the inaccurate weather forecast will pose significant influence on air traffic management. Under these uncertainties, some runway times (i.e. the estimated, targeted or calculated arrival and departure times) in ARSP will have prediction errors (Gupta et al. 2011). In the life cycle of flight operation, nearly a quarter of scheduled flights arrived more than 15 min late to its destination airport, and 70% of delay occurs in a period of 10–20 min, between aircraft start-up request and push-back (Hesselink and Paul 1998).

In China, frequent runway slot adjustments are widely applied in the ATM system, resulting in significant fluctuations and deviations during air traffic operations in the majority of hub airports. Figure 3 shows the empirical distribution of deviation from schedule (scheduling fluctuation) of a representative week at PVG. Note that the arrival deviation of a flight in Fig. 3(a) is the difference between Actual Landing Time

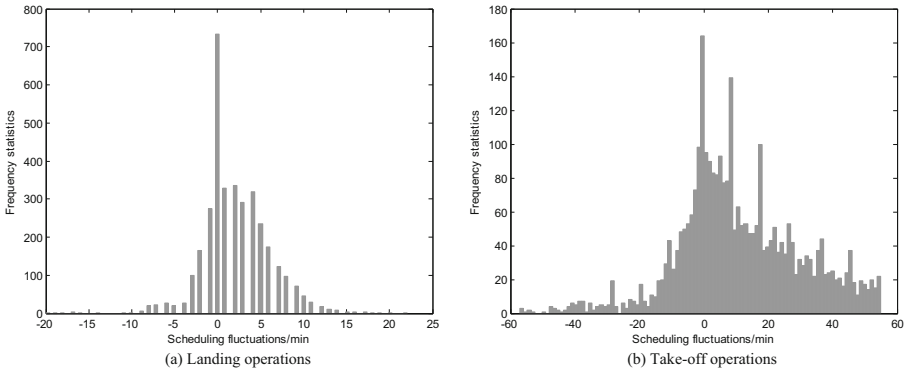


**Fig. 3** Scheduling fluctuation statistics of runway times in PVG airport

(ALDT) and Estimated Landing Time (ELDT), while the departure deviation of a flight in Fig. 3(b) is the difference between Actual Take-off Time (ATOT) and Calculated Take-off Time (CTOT). These data are analysed using frequency analysis. Figure 3(a) corresponds to the fluctuations of landing times and Fig. 3(b) shows the fluctuations of take-off times, where the latter clearly shows higher degrees of dispersion, i.e. larger

**Table 2** Framework for uncertainty tests of scheduling fluctuations

Test procedure for distribution of scheduling fluctuations:

**Input:** Historical flight data, statistic dataset sample, and set of assumed probability distributions.
**Output:** The test results of scheduling fluctuations.
**Main procedure:**

**Step 1:** Set the sample size as $n$, and $X_1, X_2, \ldots, X_n$ as the random sample of the sampling universe $X$ in PVG air traffic operations, with a corresponding observation $x_1, x_2, \ldots, x_n$.

**Step 2:** Set $X_{(1)} \le X_{(2)} \le \cdots \le X_{(n)}$ as sequential statistics of $X_1, X_2, \ldots, X_n$, and get an observation $x: x_{(1)} \le x_{(2)} \le \cdots \le x_{(n)}$ corresponding to sample $X_{(1)} \le X_{(2)} \le \cdots \le X_{(n)}$.

**Step 3:** Establish a set $\Theta$, in which the elements include probability distributions of normal, half-normal, lognormal, exponential, laplace, logistic, student, uniform, chi-squared, gamma, poisson and beta. Then conduct the test for each element in $\Theta$.

**Step 4:** For $\forall x$, we design the indicator function $I_A(\cdot)$ using a set $A = \{x_i | x_i \le x\}$:

$$I_A(x_i) = \begin{cases} 1, & x_i \in A \\ 0, & x_i \notin A \end{cases}$$

Then, for any $k \in [1, n-1] \subset N^+$, we formulate the empirical distribution function of $X$:

$$F_n(x) = \frac{1}{n}\sum_{i=1}^{n} I_A(x_i) = \begin{cases} 0, & x < x_{(1)} \\ \frac{k}{n}, & x_{(k)} \le x < x_{(k+1)} \\ 1, & x \ge x_{(n)} \end{cases}$$

Calculate the observed cumulative probability $F_n(x)$ of the observation $x$.

**Step 5:** For each element in $\Theta$, calculate the expected cumulative probability $F(x)$.

**Step 6:** Plot the point $\left(F_n(x_{(i)}), F(x_{(i)})\right)$ to analyse the relationship between observed cumulative probability and expected cumulative probability.

**Step 7:** Determine if the plotted points follow the 45-degree comparison line $y = x$; if yes, go to Step 8; otherwise, the deviations suggest the current distribution assumption is not true.

**Step 8:** Conduct Kolmogorov-Smirnov tests to the sample, and compare the P value and significance level alpha.

**Step 9:** Output the results about uncertainty tests of scheduling fluctuations.

deviations from schedules. Actually, the fluctuations described here can also reflect the slot adherence.

Furtherly, we propose a framework in Table 2 to assess the fluctuation characteristics of air traffic operations. We plot all the observed and expected cumulative probability points and determine if the assumed distribution is verified or not through cumulative probability relationship and Kolmogorov-Smirnov tests. Table 2 aims to assess the difference between the empirical and theoretical cumulative distribution functions. This is a very intuitive way to determine whether the two probability distributions are consistent.

According to the framework presented in Table 2, we conduct 12 probability distribution tests of normal, half-normal, lognormal, exponential, laplace, logistic, student, uniform, chi-squared, gamma, Poisson and beta. Due to the negative values in the sample, the fluctuation does not obey the distributions of lognormal, exponential, chi-squared, gamma, Poisson and beta. Then, Fig. 4 shows the values of observed cumulative probability and expected cumulative probability, and their relationship under the tests for the other 6 typical distributions.

From the plots in Fig. 4 and the results from Kolmogorov-Smirnov tests, we conclude that the investigated empirical scheduling fluctuations do not follow the 12 common probability distributions. Hence, most of the existing stochastic scheduling models (Sölveling 2012; Xue and Zelinski 2015; Yan et al. 2015), which assume that the uncertain input parameters have known probability distributions, are not suitable to solve the ARSP here. Inspired by Gupta et al. (2011) and Hu and Di Paolo (2008), we apply random parameters to the initial landing time $E_i^a$ and initial take-off time $E_k^d$, while not assuming certain distributions. For any ARSP instance in this paper, the runway time $E_i^a$ and $E_k^d$ are initially generated using a combination of probability set ($\eta: 20\,\%, 30\,\%, 40\%$ and $50\%$) and random interval set ($\Lambda: \pm 5, \pm 10, \pm 15$ min), representing increasing uncertainty considerations or congestion levels within 15 min. This method is similar with the time scenario settings prescribed by the discrete probability distribution (Yan et al. 2019). Table 3 presents the instance description of the uncertainty considerations in our ARSP modeling.

Take the *Case 5* in Table 3 as an example, for the initial air traffic operation data in PVG airport, we introduce the uncertainty with 30% and [−10, 10] considerations, i.e., in the planning horizon, 30% of aircraft will have new initial runway times different from their old runway times predicted, and the new times are updated in the interval [−10, 10] based on the old times.

## 3 EMOE Algorithm

Exact algorithms can get the optimal solution of ARSP, but have high computation costs (Samà et al. 2017a; Montoya et al. 2014). In order to obtain close-to-optimal solution with rational computation time, meta-heuristic algorithms are commonly applied to solve the ARSP (Sabar and Kendall 2015; Atkin et al. 2007). Firstly, we try to apply the LINGO Global Solver to solve our ARSP model, but unfortunately, there is no global optimal solution in an acceptable time of 3600 s. Considering the constrained multi-objective optimization is important from the perspective of practical

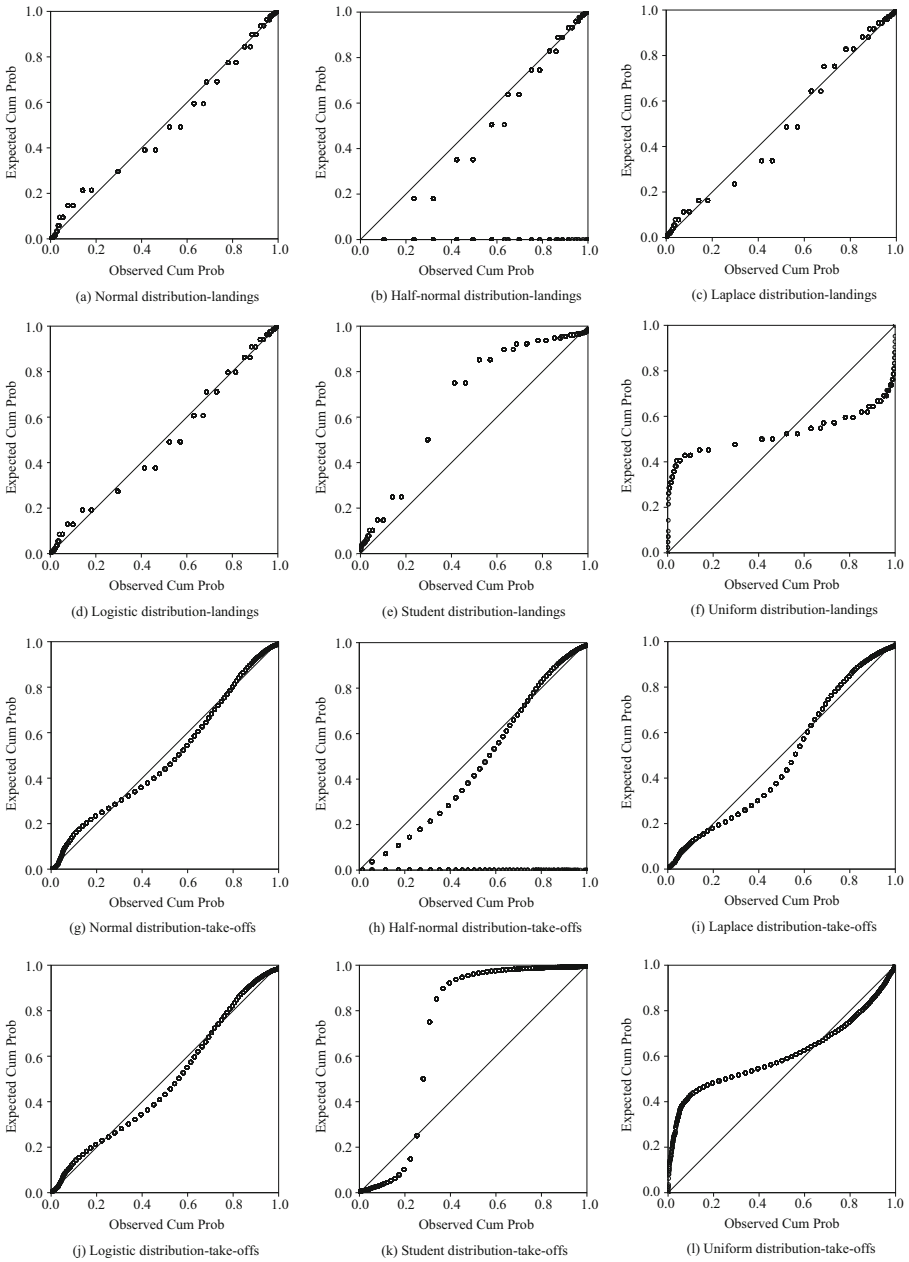


**Fig. 4** Uncertainty tests of landing and take-off fluctuations under 6 typical distributions

problem solving, we proposed an improved evolutionary algorithm EMOE with two mechanisms of ACTC and OGIS to solve the ARSP, based on the nondominated sorting genetic algorithm (Deb et al. 2002).

### 3.1 Implementation Framework

Our EMOE algorithm is inspired by a widely-used approach in the field of evolutionary biology such as inheritance, natural selection, recombination and mutation, to find a set of approximate solutions of ARSP and the make tradeoffs among delays, throughput and emissions. The basic idea and key feature of EMOE:

(1) Solution design

The solution of ARSP problem to be solved, is represented by a list of decision variables, called individual. For the individual-based meta-heuristic algorithms, extra computation costs such as the memory and time requirements exist in the binary searching. In the ARSP model, the binary decision variables $\varphi_{ij}^{a}$ and $\varphi_{kl}^{d}$ are inefficient if we use the sequence-coding methods. In order to save the cost in such cases, we adopt time-coding method in Section 3.2.1 to represent the decision variables $T_i^a$ and $T_k^d$, without using the sequence-coding.

(2) Population initialisation

Before the start of evolutionary computation, an initial set of candidate solutions is generated based on the initial runway times of landing and take-off. The quality of initial population can affect the evolution direction of the algorithm to a certain extent. Especially, some individuals in the initial population may not meet some key constraints such as Eqs. (9), (10) and (13). In order to enhance the initialisation of EMOE population, we design the ACTC mechanism in Section 3.2.2 to adaptively and controllably generate a group of initial individuals.

(3) Objective assessment

Each individual will be evaluated in the form of objectives, and the values of fitness are returned by three functions based on the optimization objectives of ARSP model. On the basis of nondominated sorting and crowding distance of NSGA-II algorithm, how to furtherly explore the evolution direction will be the key point in EMOE. In order to classify and select the best individuals from the current evolution generation, we design the OGIS mechanism in Section 3.2.3 to assess the individual quality and induce the evolution direction under different minimum schedules.

**Table 3** Instance description of the uncertainty considerations in ARSP modeling

| Cases | Uncertainty settings for the initial runway times $E_i^a$ and $E_k^d$ | | | | | | | | | | | |
|---|---|---|---|---|---|---|---|---|---|---|---|---|
| No. | 1 | 2 | 3 | 4 | 5 | 6 | 7 | 8 | 9 | 10 | 11 | 12 |
| η | 20% | 20% | 20% | 30% | 30% | 30% | 40% | 40% | 40% | 50% | 50% | 50% |
| Λ | ±5 | ±10 | ±15 | ±5 | ±10 | ±15 | ±5 | ±10 | ±15 | ±5 | ±10 | ±15 |

(4) Algorithm evolution

By removing less desired solutions from the current generation with OGIS mechanism, and producing the new generation, the population will gradually evolve to increase in

**Table 4** The pseudo code of the EMOE algorithm is depicted in Table 4

Iteration procedure of EMOE algorithm:

**Input:** Flight set, airport / airspace structure, aircraft performance, initial runway times; emission parameters, acceptable delay coefficients; Minimum separations; Minimum turnaround time; Uncertainty case No.

**Output:** The assigned runway times under different tradeoff considerations.

**Main Loop:**

**Initialization:**

(I) Set the population size $NIND$, maximum generation $MAXGEN$, evolution generation No. $g = 0$, algorithm performance matrix $OBJ$. $[NIND, 3] = size(OBJ)$ returns the sizes of each dimension of $OBJ$.

(II) Apply the ACTC mechanism to generate the initial population $I_g$, to represent the solutions with uncertainty considerations $\eta$ and $\Lambda$. $|I_g| = NIND$.

**WHILE** $g < MAXGEN$ **DO**

(I) Update $OBJ$ of $I_g$ using the three objective functions (1)-(5).

(II) Generate the parent population $P_{g+1}$ using the OGIS mechanism:

Set the strategy of inducing evolution in the OGIS mechanism for minimum scenarios

Inducing evolution strategy I: Minimum delay schedule

Inducing evolution strategy II: Minimum makespan schedule

Inducing evolution strategy III: Minimum emission schedule

Apply the strategy of preferred level identification in the OGIS mechanism

Divide all Pareto fronts of $I_g$: $F = Sort\_1(I_g)$, $F = (F_1, F_2, \dots)$.

Set $P_{g+1} = \emptyset$ and $i = 1$

**WHILE** $|P_{g+1}| + |F_i| \le NIND/2$ **DO**

Apply the strategy of single-level assessment in the OGIS mechanism

Calculate Euclidian distances of all the individuals in $F_i$

$P_{g+1} = P_{g+1} \cup F_i$

$i = i + 1$

**END WHILE**

Apply the strategy of cross-level assessment in the OGIS mechanism

Sort the solutions in $F_i$ using the partial order operator $\prec_n$: $F_i = Sort\_2(F_i, \prec_n)$

$P_{g+1} = P_{g+1} \cup F_i \left[1: \left((NIND/2) - |P_{g+1}|\right)\right]$

(III) Generate the offspring population $Q_{g+1}$ based on $P_{g+1}$:

Crossover operator: Parents $\{\rho_i^1, \rho_i^2\} \xrightarrow{u+v=1}$ Offsprings $\{\sigma_i^1, \sigma_i^2\}$, $u, v \in (0,1)$

$$\sigma_i^1 = u\rho_i^1 + (1-u)\rho_i^2$$
$$\sigma_i^2 = v\rho_i^1 + (1-v)\rho_i^2$$

Mutation operator: Inducing evolution strategy → Rand mutation model

$Q_{g+1} = NewPop(P_{g+1})$, and $|Q_{g+1}| = |P_{g+1}|$.

(IV) Combine the new $P_{g+1}$ and $Q_{g+1}$, let $R = P_{g+1} \cup Q_{g+1}$.

(V) Set $g = g + 1$, $I_g = R$.

**END WHILE**

**RETURN** the set of nondominated solutions in $F_1$

**Tradeoff:**

Set the benefit needs from different stakeholders

Assess the single and multiple objective-guided inducing strategies in the OGIS mechanism

**RETURN** the minimum delays, makespan and emissions under different tradeoff scenarios.

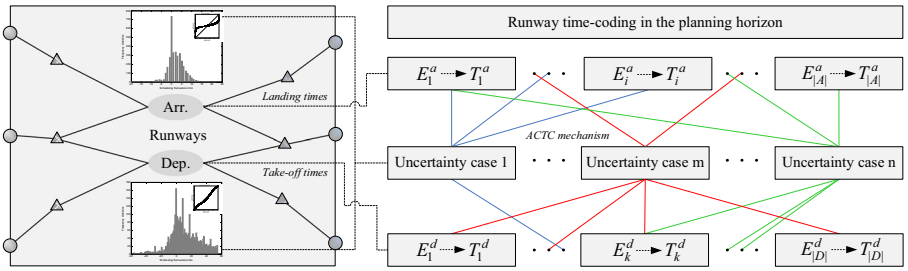


**Fig. 5** Solution representation in EMOE

fitness until the process of iteration ends on the pre-set termination condition. In order to improve the diversification of population, we adopt the crossover operation by convex combination, and the mutation model based on inducing evolution strategy in Section 3.2.4 to generate the offspring population.

The pseudo code of the EMOE algorithm is depicted in Table 4.

## 3.2 Algorithm Design

The constructive meta-heuristic provides fairly good initial solutions and maintains the population diversity. Our EMOE algorithm will seek nondominated Pareto optimal solutions of ARSP based on the assessment and evolution in each iteration. In this section, we discuss the EMOE details about solution representation, initialisation with ACTC mechanism, assessment with OGIS mechanism, and evolution with genetic operators.

### 3.2.1 Solution Representation

Note that $\varphi_{ij}^a$ and $\varphi_{kl}^d$ can be easily calculated if the values of $T_i^a$, $T_j^a$, $T_k^d$ and $T_l^d$ are definite. For example, if $T_i^a > T_j^a, \forall i,j \in A$, then $\varphi_{ij}^a = 1$; otherwise, $\varphi_{ij}^a = 0$. Hence, we design $T_i^a, \forall i \in A$ and $T_k^d, \forall k \in D$ in the form of time-coding in EMOE, which means that the assigned runway time of each aircraft is represented as a gene in the chromosome. Based on the uncertainty setting, some initial runway times of $E_i^a$ and $E_k^d$ will be updated with probability $\eta$ and random interval $\Lambda$. The solution representation is shown in Fig. 5. We design the configurations of blue, red and green lines to represent the solutions in the form of time-coding with a certain probability to update the old runway times.

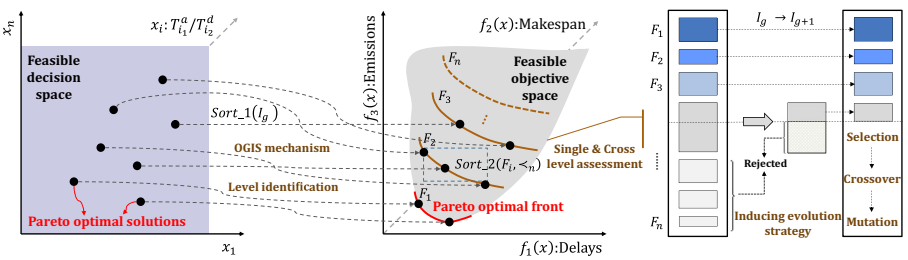


**Fig. 6** Schematic diagram of OGIS mechanism in EMOE algorithm

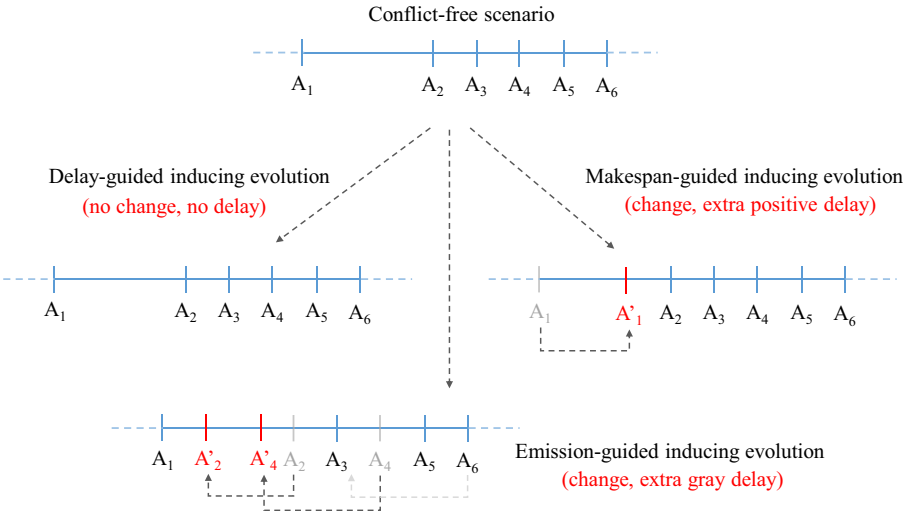


**Fig. 7** An example about the feature of inducing evolution under different minimum schedules

Obviously, the number of genes in each chromosome equals to the number of flights within the planning horizon. For example, let the assigned landing times of arrival aircraft $i$ and $j$ are 12 : 50 and 12 : 37, then the phenotypes of gene in the chromosome corresponding to aircraft $i$ and $j$ are 12.83 and 12.62, respectively. Then, the value of the decision variable $\varphi_{ij}^{a} = 1$, with the evidence that aircraft $i$ lands on the runway system after aircraft $j$.

### 3.2.2 Initialisation with ACTC Mechanism

The ACTC mechanism considers the constraints (9), (10) and (13) to initialize the population, then the factors influencing the gene values of the chromosomes in the population can be divided into three aspects with acceptable maximum delay, flight turnaround time and Hamming distance.

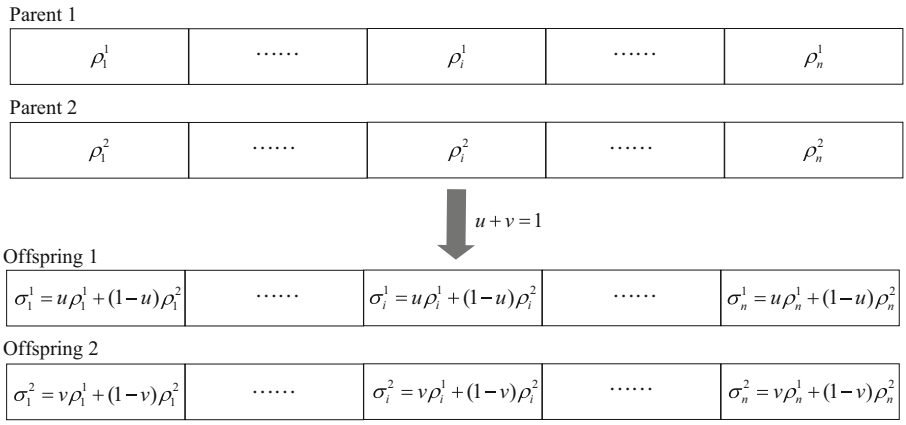


**Fig. 8** Illustration of the crossover by convex combination

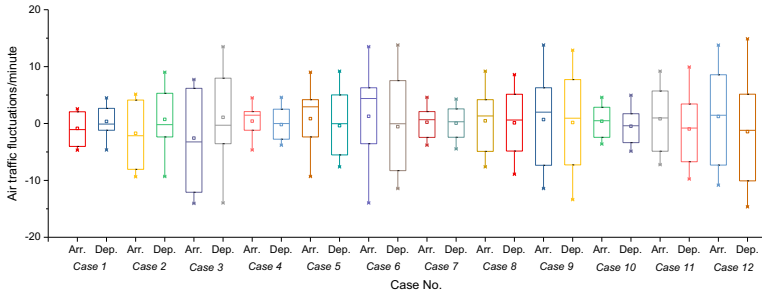


**Fig. 9** The fluctuations of landings and take-offs under 12 uncertain conditions

(1) Acceptable maximum delay

According to the constraints described by Eqs. (9) and (10), the acceptable delay of each arrival aircraft should be controlled within the interval $[-\lambda^-, \lambda^+]$. Then the phenotype of each gene for arrival is randomly created in the range of $\left[E_i^a-\lambda^-, E_i^a+\lambda^+\right]$. Similarly, the phenotype for departure aircraft is randomly created in the range of $\left[E_k^d-\lambda^-, E_k^d+\lambda^+\right]$. This can improve the individual quality in the initial population and ensure the feasibility of solutions in EMOE evolution.

(2) Flight turnaround time

According to the constraints described by Eq. (13), the difference between two runway times for each pair of connected flights (i.e., departure $k$ and arrival $i$) should be no less than a certain value $\chi_{ik}$, which can be got using the minimum turnaround time, taxi-in time and taxi-out time. This can ensure an effective connection between the preceding arrival and succeeding departure flights in any individual in the population, and reduce the costs for flight conflict resolution.

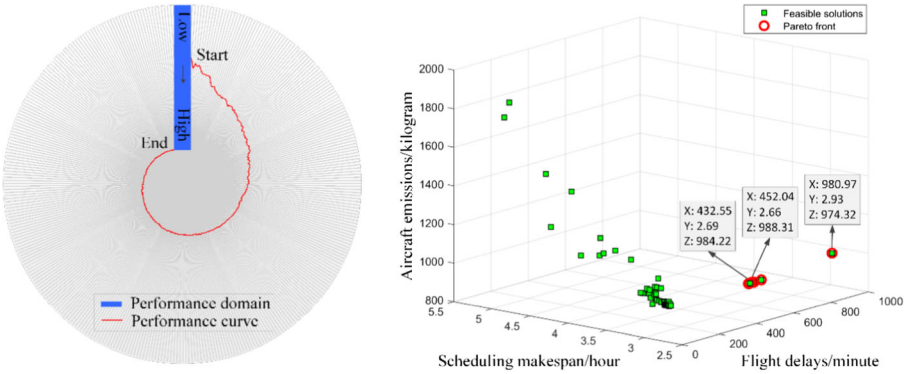


**Fig. 10** Performance of the EMOE algorithm under minimum delay schedule

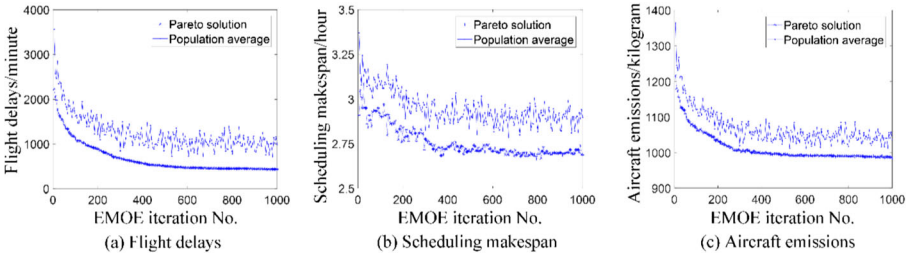


**Fig. 11** The performance of objectives under minimum delay schedule during the EMOE evolution

(3) Hamming distance

Hamming distance is one of the key metrics for measuring the difference between any two individuals, with the equal length of flight quantity, and defined as the number of gene positions at which the corresponding runway times are different. In this paper, we set the minimum Hamming distance of any two individuals as the half of flight quantity. This can improve the diversity of individuals in the initial population, and increase the difference between feasible solutions, and then avoid the premature convergence of algorithm.

### 3.2.3 Assessment with OGIS Mechanism

According to the three optimization objectives seen in Eqs. (1)–(5), the fitness functions of our algorithm are designed in Eqs. (14)–(16).

$$f_1 = \left\{ \left( \sum_{i \in A} \left| T_i^a - E_i^a \right| + \sum_{k \in D} \left| T_k^d - E_k^d \right| \right) + \varepsilon \right\}^{-1} \tag{14}$$

$$f_2 = N - \left\{ \max\left( T_{|A|}^a, T_{|D|}^d \right) - \min\left( T_1^a, T_1^d \right) \right\} \tag{15}$$

**Table 5** Comparison of optimization objectives for each type of instance

| Instance | | Delays/m | | Makespan/h | | Emissions/kg | |
|---|---|---|---|---|---|---|---|
| No. | Type | Best | Average | Best | Average | Best | Average |
| 1 | EMOE-D | **432.55** | 669.26 | 2.69 | 2.76 | 984.22 | 1013.46 |
| 2 | EMOE-M | 546.12 | 742.93 | **2.62** | 2.71 | 1001.00 | 1019.84 |
| 3 | EMOE-E | 723.41 | 833.35 | 3.07 | 2.85 | **919.90** | 1007.17 |
| 4 | NSGA-II-D | **441.32** | 676.39 | 2.70 | 2.78 | 981.69 | 1012.59 |
| 5 | NSGA-II-M | 496.89 | 676.39 | **2.67** | 2.78 | 985.81 | 1012.59 |
| 6 | NSGA-II-E | 668.92 | 676.39 | 2.73 | 2.78 | **974.33** | 1012.59 |
| 7 | GA-F-W | **611.43** | 837.18 | **2.71** | 2.78 | **1006.34** | 1032.97 |
| 8 | FCFS | **1348.04** | – | **2.75** | – | **1125.77** | – |

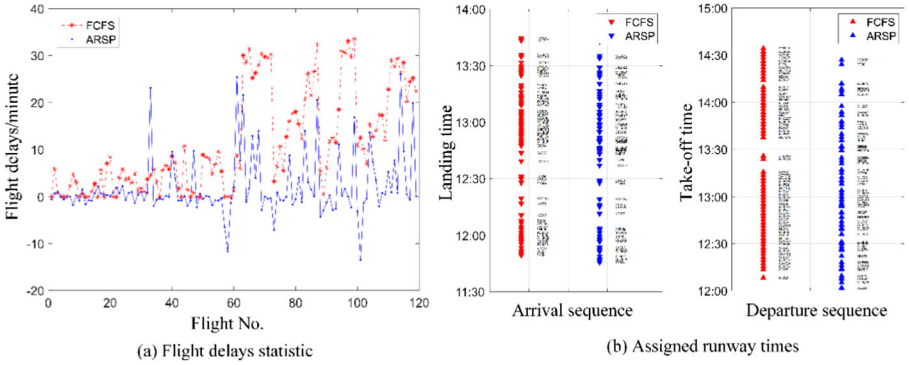


**Fig. 12** Distribution of flight delays and assigned runway times using FCFS and ARSP

$$f_3 = \left\{ \begin{array}{l} \sum_{i\in A}\sum_{m\in P}\left(P_i^a f_i^1 e_i^{m,1} + Q_i^a f_i^2 e_i^{m,2}\right) + \\ \sum_{k\in D}\sum_{m\in P}\left(Q_k^d f_k^2 e_k^{m,2} + P_k^d f_k^3 e_k^{m,3}\right) \end{array} \right\}^{-1} \tag{16}$$

Where $\varepsilon \in [0.5,1.5]$ denotes any real number, $N$ denotes a large number as doubling the sum of planning horizon and acceptable maximum delay.

The OGIS mechanism considers the Eqs. (1)–(5) to measure the individual performance of each objective, then we can produce the top $NIND/2$ best solutions from each generation as the parent population $P_{g+1}$ in the next evolution. Figure 6 shows the schematic diagram of OGIS mechanism to identify and assess the Pareto fronts and nondominated solutions. The OGIS mechanism can be divided into four perspectives: preferred level identification, single-level assessment, cross-level assessment and inducing evolution strategy.

(1) Preferred level identification

The preferred level identification focuses on all the individuals in each population. According to the performance matrix $OBJ$, the evolutionary individuals in each iteration can be divided into different levels with priority. Then we can obtain the preferred individuals at each level and the dominant relationships among different levels. First, we calculate all the performance indicators $OBJ(1:NIND, 1:3)$ corresponding to flight delays, scheduling makespan and aircraft emissions. For any individual $p$ in the population $I_g$, compare its performance indicators with those of all the other individuals $q$ ($q \in I_g, q \neq p$). Then we analyse the dominate relationship between $p$ and $q$, and get the dominated set $S_p$ and parameter $n_p$. Finally, The solutions with $n_p = 0$ will be selected into the first level $F_1$, and similarly for the other solutions in the levels $F_2$, $F_3$, … based on the dominated sets of all the individuals.

(2) Single-level assessment

The single-level assessment focuses on all the individuals with the same $n_p$ in each level. According to the individuals in level $F = (F_1, F_2, \ldots)$, we can analyse the density

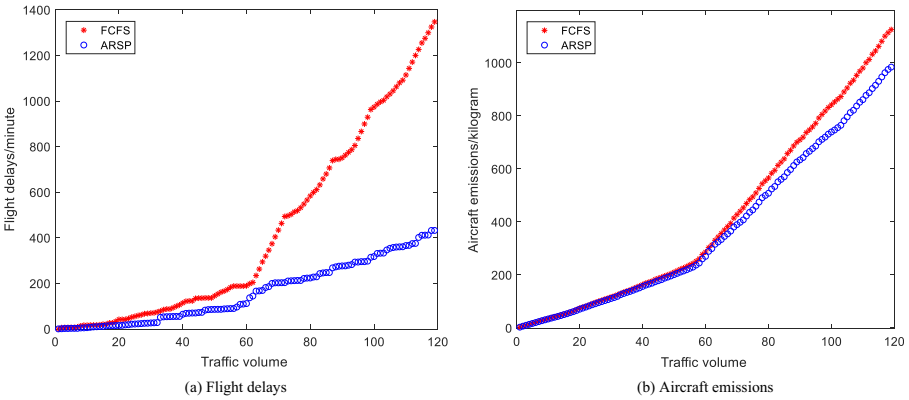


**Fig. 13** Flight delays and emissions vs. traffic volume using FCFS and ARSP

of solution distribution around each individual, and assess the preferred sequence in level $F_i$. First, we sort all the individuals in level $F_i$ in ascending order based on the flight delays, scheduling makespan and aircraft emissions. Then the Euclidian distance for each individual in level $F_i$ can be calculated based on the multiple objectives in the three dimensional space. During each evolution, the Euclidian distances are mainly decided by the performance matrix *OBJ*. In addition, for each evolution iteration, the single-level assessment will focus on the *OBJ*(:, 1) under minimum delay schedule, *OBJ*(:, 2) under minimum makespan schedule, and *OBJ*(:, 3) under minimum emission schedule. Finally, we can get the preferred No. of each individual in $F_i$.

(3) Cross-level assessment

The cross-level assessment focuses on the individuals with the top *NIND*/2 best performance in each population. Here we use the partial order operator $\prec_n$ introduced by Deb et al. (2002) to get the preferred No. of all individuals in the population $I_g$. The guiding rule is: for the same level, we select the solution with larger Euclidian distance; but for different levels, the lower level will be selected.

(4) Inducing evolution strategy

Based on the preferred level identification, single-level assessment, and cross-level assessment, we adopt different inducing evolution strategies from the single-objective-guided and multiple-objective-guided perspectives. Figure 7 shows an example about the feature of inducing evolution under different minimum schedules for a segment of an individual. Once the sequence has been optimized as a conflict-free sequence at a certain generation during the evolution, then different inducing strategies will make the following evolution go to different directions.

For the conflict-free scenario in Fig. 7, under the delay-guided inducing strategy, there will be no delay, and the makespan equals to $|A_1A_6|$. However, under the makespan-guided inducing strategy, the $A_1$ will be adjusted to $A'_1$, there will be extra positive delay, and the makespan equals to $|A'_1A_6|$. Under the emission-guided inducing strategy, the $A_2$ may be adjusted to $A'_2$, and the $A_4$ may be adjusted to $A'_4$. It is also

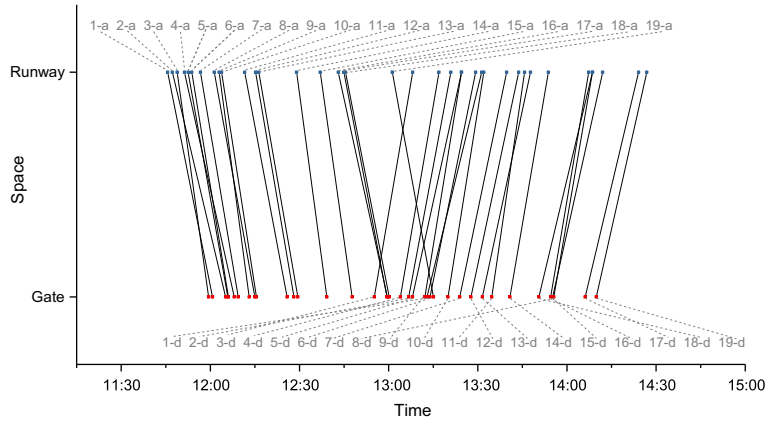


**Fig. 14** The spatial-temporal resource flow of connected flights

possible to perform similar operations on $A_3$, $A_5$ or $A_6$. Then there will be extra gray delays. Note that these strategies will only be applied in the scenario with no conflict in the sequence but we want to furtherly reduce the makespan and emissions. Based on the above inducing evolution strategies, we comprehensively compare the evolutionary direction, and assess the optimization results, then we will make tradeoffs among multiple performance indicators under different inducing evolution strategies presented in Section 5.2.

### 3.2.4 Evolution with Genetic Operators

Besides the presented inducing evolution strategies, for the top *NIND*/2 best individuals got from the OGIS mechanism, we use the genetic operators of convex combination crossover and rand mutation (Hamid et al. 2019; Michalewicz 1996) to produce the other *NIND*/2 offsprings. Let the gene codes on position $i$ in the old two chromosomes are $\rho_i^1$ and $\rho_i^2$, then the gene codes in the new chromosomes $\sigma_i^1$ and $\sigma_i^2$ can be represented in Table 4. Figure 8 gives an example to illustrate this type of crossover.

The crossover operation by convex combination encourages diversification of research while remaining close to the information carried by the two parents or exploration of non-visited areas in the search space, and finding new solutions different from those encountered before. It can ensure that both offsprings are feasible if both parents are. The rand mutation operator changes the value of chosen gene with uniform random value selected with the window of acceptable delay shown in the Eqs. (9) and (10). Finally, the next evolution population is fully formulated, and the next iteration begins.

## 4 Case Study and Results

A case study of ARSP in PVG airport is conducted for optimizing the runway sequences and times under segregated parallel operations. We report the computational

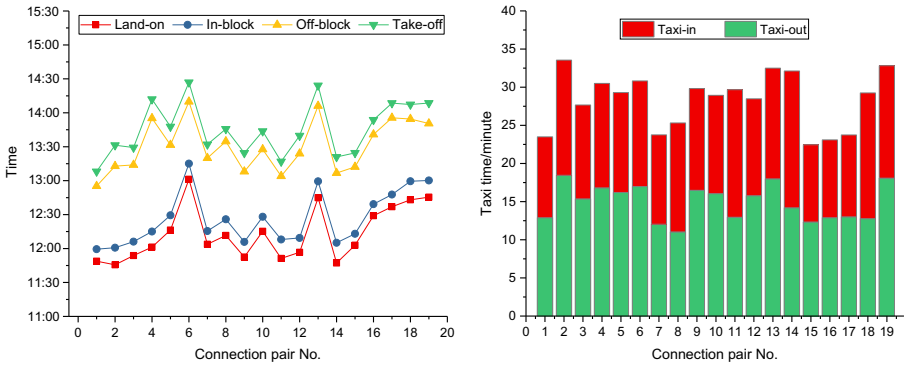


(a) Runway and gate time (b) Taxi time

**Fig. 15** Key event times of each pair of connected flights

performance of our method, and present the comparison results with some meta-heuristics and FCFS.

### 4.1 Experimental Environment

The total number of arrival and departure aircraft within the planning horizon 12:00–13:59 are 56 and 63, respectively. The acceptable maximum delay and gray delay are 30 and 20 min, respectively. The minimum turnaround time is 65, 55 and 45 min, respectively, based on the aircraft type of heavy ('H'), medium ('M') and light ('L'). According to the settings of *Cases 1–12* in Table 3, Fig. 9 presents the fluctuations of landings and take-offs under 12 uncertain conditions.

The ARSP model and EMOE algorithm are integrated with Airport and Airspace Simulation and Evaluation System (AASES) developed by National Key Laboratory of Air Traffic Flow Management in China. The AASES consists two modules: airport module and airspace module, which aim to simulate the ground and TMA movements. The parameters such as taxiing time, TMA operation time, i.e., $Q_i^a, Q_k^d, P_i^a, P_k^d$, can be calculated by the airport module and airspace module. The EMOE parameters: the population size in each generation is 100, the maximum evolution number of generation is 1000, and the coding length of each individual is 119. The minimum Hamming distance is 60. The crossover and mutation probability are 0.7 and 0.2, respectively.

### 4.2 Computational Performance

The EMOE is coded in Matlab 2016 and run on a PC with a 8-Core, 3.60 GHz and 16.0 GB RAM. Computational experiments show that the population performance is approaching gradually to the optimum direction with the evolution increases, and the Pareto optimal solutions are rapidly searched in the ARSP decision space. Without loss of generality, we use *Case 12* under minimum delay schedule to present the EMOE performance, and compare it with some meta-heuristics.

**Table 6** The gate time difference and runway time difference of each pair of connected flights

| Arr-Dep Pairs | | Gate times | | | Runway times | | | Turnaround times /minute | |
|---|---|---|---|---|---|---|---|---|---|
| No. | Type | In-block | Off-block | Diff. | Land-on | Take-off | Diff. | Min. | Est. |
| 1 | M | 11.99 | 12.92 | 0.93 | 11.81 | 13.13 | 1.32 | 55 | 56 |
| 2 | M | 12.01 | 13.21 | 1.20 | 11.76 | 13.52 | 1.76 | 55 | 72 |
| 3 | H | 12.10 | 13.23 | 1.13 | 11.90 | 13.49 | 1.59 | 65 | 68 |
| 4 | M | 12.25 | 13.92 | 1.67 | 12.02 | 14.20 | 2.18 | 55 | 100 |
| 5 | M | 12.49 | 13.53 | 1.04 | 12.27 | 13.80 | 1.52 | 55 | 62 |
| 6 | M | 13.25 | 14.16 | 0.91 | 13.02 | 14.45 | 1.43 | 55 | 55 |
| 7 | M | 12.26 | 13.33 | 1.08 | 12.06 | 13.53 | 1.47 | 55 | 65 |
| 8 | M | 12.43 | 13.58 | 1.15 | 12.19 | 13.76 | 1.57 | 55 | 69 |
| 9 | M | 12.10 | 13.13 | 1.04 | 11.88 | 13.41 | 1.53 | 55 | 62 |
| 10 | M | 12.47 | 13.46 | 0.99 | 12.25 | 13.73 | 1.48 | 55 | 60 |
| 11 | M | 12.13 | 13.07 | 0.93 | 11.85 | 13.28 | 1.43 | 55 | 56 |
| 12 | M | 12.16 | 13.40 | 1.24 | 11.94 | 13.66 | 1.72 | 55 | 75 |
| 13 | M | 12.99 | 14.10 | 1.11 | 12.75 | 14.40 | 1.65 | 55 | 67 |
| 14 | M | 12.09 | 13.11 | 1.03 | 11.79 | 13.35 | 1.56 | 55 | 62 |
| 15 | M | 12.22 | 13.20 | 0.99 | 12.05 | 13.41 | 1.36 | 55 | 59 |
| 16 | M | 12.65 | 13.68 | 1.03 | 12.48 | 13.90 | 1.41 | 55 | 62 |
| 17 | M | 12.80 | 13.93 | 1.13 | 12.62 | 14.14 | 1.53 | 55 | 68 |
| 18 | M | 12.99 | 13.91 | 0.92 | 12.72 | 14.12 | 1.40 | 55 | 55 |
| 19 | M | 13.00 | 13.84 | 0.84 | 12.76 | 14.14 | 1.39 | 55 | **50** |

#### 4.2.1 Multi-Objective Optimization Performance

Figure 10 illustrates the performance of EMOE. The running time can be controlled within 10 s/aircraft (including data processing, schedule formulation, performance tradeoff and computational visualization), when the flight quantity is 119.

It has a significant reduction of computation cost comparing with the method proposed by Bojanowski et al. (2011) and Malik et al. (2016) after expanding their sample using a linear incremental function. A large number of experiments show that the running time of schedule formulation can be generally controlled within 6 s/aircraft. Hence, the EMOE can satisfy the decision making needs in multi-runway systems on the pre-tactical or tactical levels.

Figure 11 shows the changes of delays, makespan and emissions in the EMOE evolution. With the EMOE evolution generation increasing, the delays in Fig. 11(a) has decreased from 2338.90 min in the first evolution to 432.55 min in the last evolution, and tends to the best performance at the maximum generation. Similary, the emissions in Fig. 11(c) has decreased from 1231.34 kg to 984.22 kg. However, the makespan in Fig. 11(b) has an overall decreasing trend with some fluctuated changes, which reveals a fact that when the flight delay reaches to the minimum value, the makespan may be larger than the minimum makespan. As the iteration goes to the maximum generation,

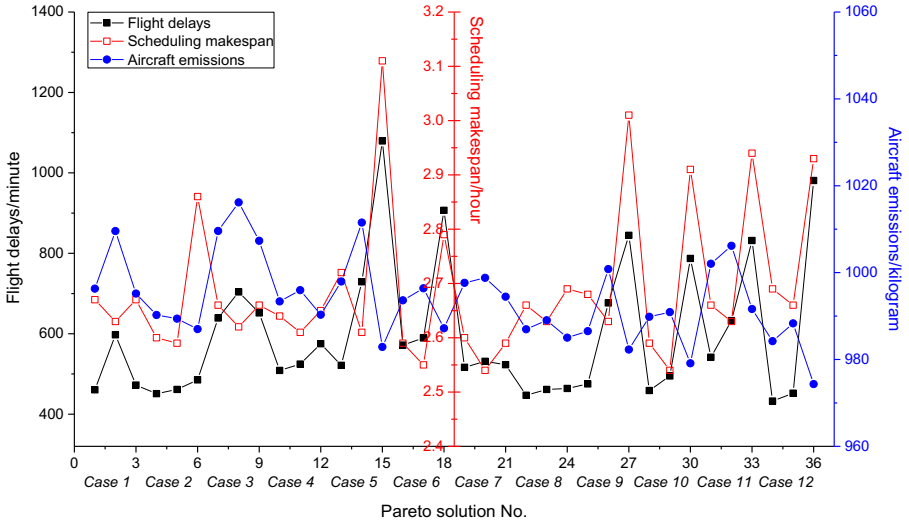


**Fig. 16** Delay, makespan and emission tradeoffs under 12 uncertain conditions

the delays and emissions tends to the minimum, and the makespan can be controlled to about 2.7 h.

It can be obviously seen that the convergence performance, which corresponds to the nodominated Pareto optimal solutions, is significant, although there are some fluctuations among different runway time individuals in each evolutionary generation. Note that the results in Fig. 11 is just an illustration of solution exploration under the minimum delay schedule, and there will be significant difference under the minimum makespan and emission schedules presented in Section 5.2.

#### 4.2.2 Comparison with some Meta-Heuristics and FCFS

We investigate the effectiveness of EMOE in contrast with the performance of some meta-heuristics, and also the FCFS. Table 5 shows the performance of each objective for *Case 12* under a serial of instances. The instances are designed as follows:

(I). EMOE-D: Optimize the multi-objective using EMOE with delay-guided induction;
(II). EMOE-M: Optimize the multi-objective using EMOE with makespan-guided induction;
(III). EMOE-E: Optimize the multi-objective using EMOE with emission-guided induction;
(IV). NSGA-II-D: Optimize the multi-objective using NSGA-II, and select the Pareto solutions with minimum delays;
(V). NSGA-II-M: Optimize the multi-objective using NSGA-II, and select the Pareto solutions with minimum makespan;
(VI). NSGA-II-E: Optimize the multi-objective using NSGA-II, and select the Pareto solutions with minimum emissions;

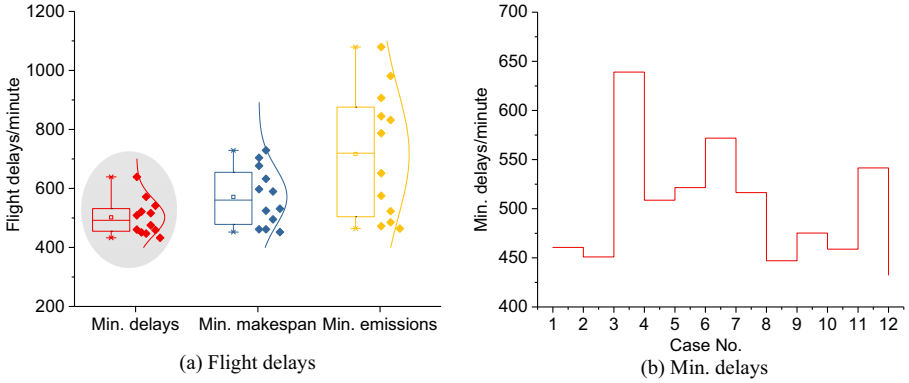


**Fig. 17** Distribution of delay values under 3 minimum scenarios and 12 uncertainty cases

(VII). GA-F-W: Optimize the fairly weighted multi-objective using the general genetic algorithm;
(VIII). FCFS: First Come First Served strategy without other optimization.

Columns 1–2 present the types of the EMOE, other meta-heuristic algorithms and FCFS. Columns 3–4, 5–6, and 7–8 report the best / average performance of delays, makespan and emissions objectives, respectively. The best values are marked in bold regarding each type (i.e., EMOE, NSGA-II, GA, and FCFS) of algorithms. Note that the average values regarding NSGA-II in each column is equal, because we get three best Pareto solutions from one experiment with the same final population. For the 119 aircraft scheduling in Table 5, FCFS algorithm shows the worst performance for ARSP except the makespan, and then the GA-F-W algorithm with large emissions. The bold values of each objective using the FCFS and GA-F-W are significantly larger than those using the NSGA-II and EMOE. The EMOE-D, EMOE-M, EMOE-E have the best performances on minimizing the delays, makespan and emissions, respectively. However, the EMOE-M and EMOE-E minimize the makespan and emission at the expense of increasing the (gray) delays. Therefore, the EMOE algorithms have overall advantages to make flexible performance tradeoffs for ARSP.

### 4.3 Numerical Results

Considering the results under 12 uncertainty cases in Table 3 are similar to describe, in this section we take the *Case 12* for an instance to compare the results of different runway scheduling strategies, and then analyse interactions between arrivals and departures during turnaround processes.

#### 4.3.1 ARSP Vs. FCFS

We take the FCFS as a baseline, and compare it with the ARSP. Figure 12(a) shows the distribution of delays using FCFS and ARSP. The maximum delays of single arrival and departure using ARSP are 23.12 and 26.27 min, respectively. And the departure delays occupy a larger part in all the delays. Additionally, we also analyse the makespan

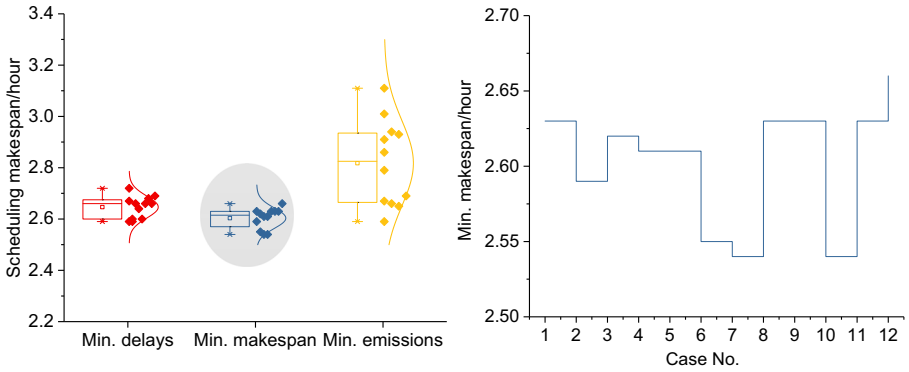


(a) Scheduling makespan (b) Min. makespan

**Fig. 18** Distribution of makespan values under 3 minimum scenarios and 12 uncertainty cases

based on the runway sequences and times in Fig. 12(b). The scheduling makespans calculated by FCFS and ARSP are 2.75 and 2.69 h, respectively. Compared with the FCFS, the ARSP cannot get a further decrease in makespan, as the runway system is reaching its maximum capacity. Actually, for such saturated airport operational environment, the significance of ARSP lies in the reduction of delays and emissions.

The maximum gray delays of single arrival and departure aircraft using ARSP are 2.30 and 13.49 min, respectively. In order to analyse the ARSP performance in reducing delays, we conduct some punctuality analysis from different views. If we define the on-time flight as the aircraft with the absolute value of delay no more than 15 min, then the quantity of aircraft that is not on-time under FCFS and ARSP is 38 and 7, respectively, and the punctuality rate can be increased by 26.05%. Additionally, if we enlarge the statistic range from 15 to 20 min, the quantity of aircraft that is not on time under FCFS and ARSP is 30 and 5, respectively, and the punctuality rate can be increased by 21.01%. The proposed method can significantly improve the on-time performance by controlling the aircraft delays in a smaller range. The EMOE allows a small amount of large delays in ARSP, because we find that it is possible to minimize the total delays at the expense of delaying a small number of flights for acceptable longer times. If we set the acceptable maximum delay parameters $\lambda^-$ and $\lambda^+$ to smaller values, the EMOE can control the delay of each flight to a certain smaller level.

Figure 13 compares the delays for scenarios involving different numbers of aircraft. It can be seen that the reduction of delays using ARSP and FCFS can be divided into two branches with a truncation point of 61. When the traffic volume is less than 60, there is little benefit over the FCFS strategy in minimizing the delays and emissions. However, the ARSP does perform better than the FCFS under a high traffic volume more than 60. When the air traffic demand reaches to the capacity limit (around 60 aircraft per hour here), the flight delays in PVG airport will significantly arise. Under the FCFS, the existing capacity is not fully utilized, then the delays will increase drastically. However, under the ARSP, the flight sequences and runway times will be optimized to make the demand capacity balance, then the delays will not increase drastically.

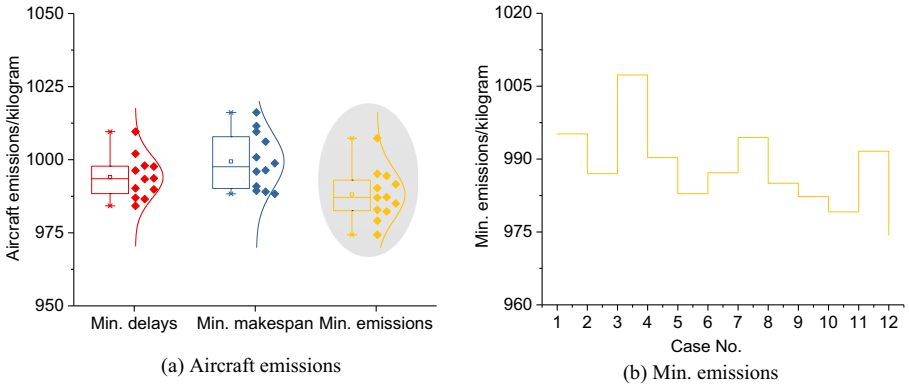


(a) Aircraft emissions (b) Min. emissions

**Fig. 19** Distribution of emission values under 3 minimum scenarios and 12 uncertainty cases

In Fig. 13(a), for the scenario with 119 flights, the average delay per flight has decreased from 11.33 (FCFS) to 3.63 (ARSP under minimum delay schedule) min. The reason for such a significant reduction is a commonly confirmed fact that the flight timetable formulation of PVG airport at the strategic level is unreasonable, the FCFS will result in some inevitable resource conflicts and flight delays at the pre-tactical or tactical levels. Moreover, the average delay differs by 1.30 (volume = 60 flights) and 7.70 (volume = 119 flights) min. Hence, the ARSP is shown to successfully reduce the delays compared to FCFS, and the effectiveness is more pronounced for high-demand scenarios (>60 flights). However, the delays under minimum makespan schedule is 546.12 min, this reveals the importance of tradeoffs among different performance indicators. Figure 13(b) regarding emissions has a similar overall trend as Fig. 13(a). However, unlike the delays, the ARSP proves less effective in reducing emissions in the first branch (<=60 aircraft), as the emissions are 286.37 (FCFS) and 270.08 (ARSP) kg, respectively. For a total of 119 flights, the emissions are 1125.77 (FCFS) and 984.22 (ARSP) kg, respectively. Due to the key influence of taxiing time and route operation time, the emissions cannot be significantly reduced only through reducing the delays.

### 4.3.2 Turnaround Analysis

Considering the constraint (13) in Section 2.3, the runway time difference of each pair of connected arrival and departure flights is designed to be no less than the minimum connection coefficient $\chi_{ik}$. Unlike the hard constraints, e.g., the minimum separation constraints, the turnaround constraint is a soft constraint in our ARSP model, which can be easily resolved by the AASES platform. In this section, we analyse the performance of turnaround and ground movements for 19 pairs of connected flights in the planning horizon. Figure 14 shows the spatial-temporal resource flow of connected flights through a macrscopic description of space and time resources.

For any $i \in \{1, 2, \ldots, 19\}$, the marks "*i-a*" and "*i-d*" in Fig. 14 mean the *i-th* pair of connected flights including the arrival *i* and departure *i*. The arrivals (departures) are represented by the lines pointing from blue (red) points to red (blue) points, with relevant measurable land-on (off-block) and in-block (take-off) times. Except the

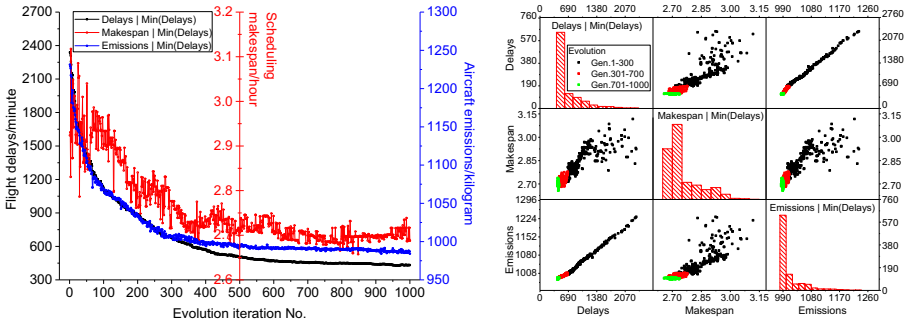


(a) Performance change (b) Correlation analysis

**Fig. 20** Tradeoffs among delay, makespan and emission under minimum delay schedule

"3-*a*" and "3-*d*" being type 'H' with a minimum turnaround time of 65 min, the type of other 18 connected arrivals and departures are 'M' with 55 min. Figure 15 shows the times of key events, such as the land-on, taxi-in, in-block of arrivals and off-block, taxi-out, take-off of departures, for each pair of connected flights.

Table 6 illustrates the values of gate times and runway times, and the differences between off-block and in-block, between take-off and land-on for each pair of connected flights. As presented in Section 3.2.1, the values of times are listed in the form of gene phenotypes in ARSP solutions. For example, the in-block time of arrival in Pair No.1 is 11.99 means it reaches the designated gate at 11:59. Similarly, the take-off time of departure in Pair No.1 is 13.13 means it leaves the ground at 13:08.

From the last two columns of illustrated turnaround times in Table 6, we can see that 18 pairs, Nos. 1–18, of connected flights are expected to finish the turnaround service according to the input coefficients in our ARSP model, with estimated turnaround times no less than the minimum. However, a time advance of 5 min is suggested for the Pair No.19 during its turnaround process, which can be easily operated by airlines and airport ground services. That is to say, 94.7% of soft constraints are met. This is rational and applicable in practice that some airlines have historically tried to turn around aircraft in as little as 30 min at the gate. Actually, the turnaround process in Chinese airports has been accelerated in the past few years, and the minimum turnaround times have been continuously optimized in relevant regulations. The emphasis on quick turnaround reduces the conflicts of gates and terminal space at busy airports, and then enhance the efficiency of aircraft and passengers.

## 5 Tradeoff Analyses

As a multi-objective optimization problem, the ARSP model and EMOE algorithm can get a set of nondominated Pareto optimal solutions from different perspectives of stakeholders. We conduct a comprehensive analysis and comparison for the tradeoffs among delays, makespan and emissions under some different scenarios in terms of uncertain conditions and minimum schedules.

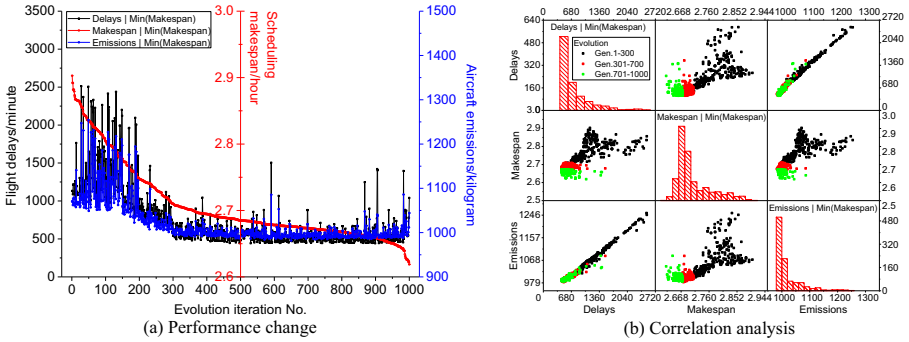


**Fig. 21** Tradeoffs among delay, makespan and emission under minimum makespan schedule

### 5.1 Tradeoffs under Uncertain Conditions

We consider 12 cases with different combinations of probability and random interval in Table 3, and then conduct studies of scheduling a sequence of 119 flights described in Section 4.1. Figure 16 shows the tradeoffs among delays, makespan and emissions under different uncertain conditions. Note that the gray delays are also considered in the statistics. For each case in Fig. 16, the tradeoffs represent three nodominated Pareto optimal solutions and minimum performance indicators. Take *Case 1* as an example, the solutions searched when minimizing the delays, makespan and emissions, respectively, are S1 = (460.61, 2.67, 996.30), S2 = (597.30, 2.63, 1009.57) and S3 = (472.23, 2.67, 995.17). Obviously, there are tradeoffs among delays, makespan and emissions, and the minimum values of the three objectives are 460.61 min, 2.63 h and 995.17 kg, respectively.

Air transport stakeholders are suggested to select the first black / second red / third blue points as the preferred delays / makespan / emissions results. Some large fluctuations of the distribution of Pareto optimal solutions exist when comparing the results from different uncertain conditions. However, there are no obvious rules or guidelines to follow, because the difference of any two uncertainty cases are focused on the parameters of probability and random interval, and the relationship between parameter setting and minimum values are not significant. Actually, a large probability or random interval of uncertainty consideration, which only reflects large fluctuations of initial runway times, does not means large delays, makespan or emissions.

We also investigate the performance tradeoffs under different inducing evolution strategies. Figure 17 reveals that the delays under minimum makespan schedule does differ from that under minimum delay schedule. This means that the benefit from minimizing the makespan comes at the expense of increasing the delays. While minimizing the emissions, the delays differ very much from the minimum delays. The reason is that some existing gray delays can increase the total delays, but decrease the emissions. Due to the fact that small deviation from the initial times will make a small makespan, the makespan under minimum delay schedule does not differ very much from that under minimum makespan schedule in Fig. 18. Similar with Fig. 17, while minimizing the emissions, the makespan also differ from the minimum makespan, due to the existence of gray delays. Regarding the emissions in Fig. 19,

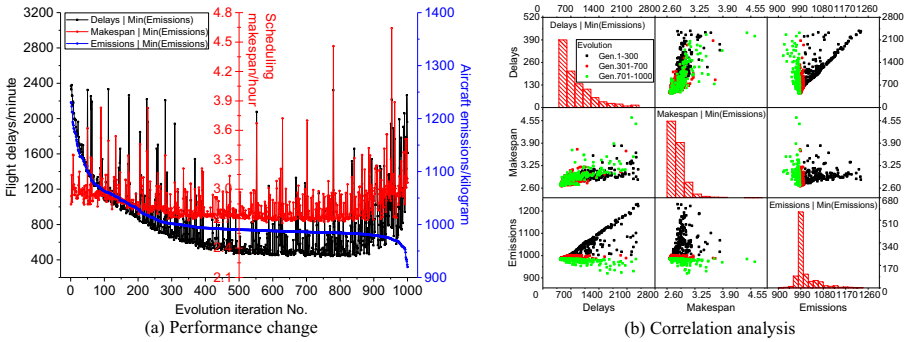


**Fig. 22** Tradeoffs among delay, makespan and emission under minimum emission schedule

the values of minimum delay schedule does not obviously differ from the minimum emissions, and the minimum makespan schedule may result into larger emissions.

In a word, the uncertainty characteristics of air traffic operations is important in ARSP modeling and real practice, and different uncertainty considerations are significantly related to the performance metrics of delays, makespan and emissions. In real practice at hub airport systems, the uncertainty parameters can be flexibly set based on the decision needs and demand characteristics.

### 5.2 Tradeoffs under Different Minimal Schedules

We investigate the tradeoffs among delays, makespan and emissions under different minimum schedules. Without loss of generality, we take the *Case 12* for analysis. Figures 20, 21 and 22 illustrate the tradeoffs and correlations among delays, makespan and emissions under the minimum delay /makespan /emission schedule during the EMOE evolution.

The step-by-step changes of delays in Fig. 20(a) differ from those of makespan, but are similar with those of emissions, as the delays continue to decrease. Then all the values are analysed by frequency analysis, and reperesented by the black, red and green points for the generation Nos. 1–300, 301–700 and 701–1000 in Fig. 20(b), respectively. Here we use the label *i-j* to indicate the subgraph located in row *i* and column *j*. The subgraphs 1–3 and 3–1 reveal that the linear correlation between delays and emissions under minimum delay schedule is strong. The reason is that the delay has a significant contribution in the calculation of emissions when minimizing the delays, while the taxiing time and TMA operation time are relatively fixed. The subgraphs 1–2, 2–1, 2–3 and 3–2 in Fig. 20(b) show that the correlations between delays / emissions and makespan are not significant, due to the fluctuations of makespan, obviously seen in Fig. 20(a).

According to Fig. 21(a), the changes of delays and emissions differ very much from those of makespan, as the makespan continues to decrease. It can be easily seen that a makespan of 2.7 h is a rational satisfactory value for decision-making reference. The attempt to get a larger reduction on makespan does not work to furtherly reduce the delays and emissions. The linear correlation between delays and emissions in Fig. 21(b) under minimum makespan schedule is strong, while the correlations between delays / emissions and makespan are not significant. The step-by-step changes of delays and

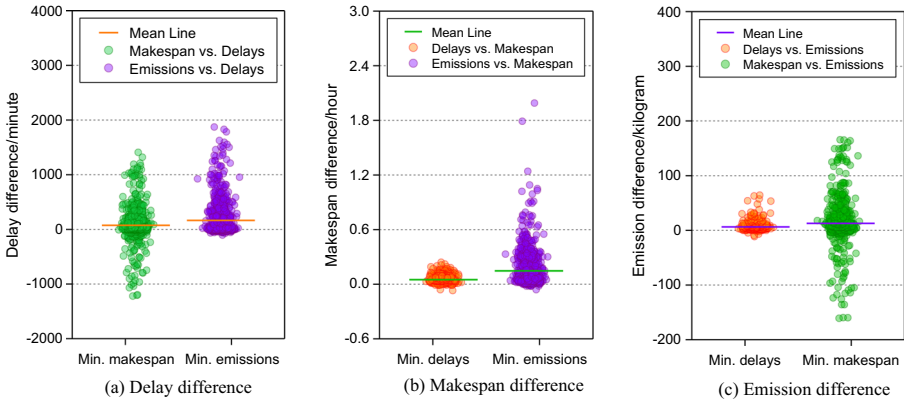


**Fig. 23** The delay, makespan and emission differences under multiple minimum schedules

makespan in Fig. 22(a) differ very much from those of emissions, as the emissions continue to decrease. The delays and makespan fluctuate within a large range when the emissions are rapidly approaching the minimum. The subgraphs 1–2, 2–1, 1–3, 3–1, 2–3 and 3–2 in Fig. 22(a) reveal that there are no significant correlations among delays, makespan and emissions under minimum emission schedule.

Figure 23 investigates the delay / makespan / emission tradeoffs under the minimum delay, makespan and emission schedules. Regarding the delays, the mean differences and standard deviations between minimum makespan / emission and delay schedule are 73.67 / 164.09 min and 267.26 / 296.49 min. The mean makespan differences and standard deviations between minimum delay / emission schedule and minimum makespan schedule are 0.05 / 0.15 h and 0.04 / 0.18 h. Additionally, the mean emission differences and standard deviations between minimum delay / makespan schedule and minimum emission schedule are 6.30 / 12.68 kg and 5.99 / 34.02 kg.

To summarize the above results, the tradeoffs among delays, makespan and emissions are obviously different under different minimum schedules. We can conclude that under the minimum delay schedule, the emissions values are also close to the minimum, while the makespan values have an overall decreasing trend with a lot of fluctuations. Under the minimum makespan schedule, both delays and emissions are not close to the minimum and have obvious fluctuations. Similarly, under the minimum emission schedule, the delays and makespan are not close to the minimum and also with fluctuations. Hence, the tradeoff analyses suggest that the minimum delay schedule is the best choice to make satisfactory tradeoffs among delays, makespan and emissions in the real practice. The fact is the makespan and emissions can also approach the minimum when we minimizing the delays, supported by the orange points in Figs. 23(b)-(c). In real practice at high density traffic airports, minimizing the makespan to an irrationally too small range is not a desirable measure to improve the performance of air traffic operations, resulting into high values of delays and emissions due to the saturation. The efficient solution to improve the airport performance is accommodating more demand under the existing capacity, rather than reducing the scheduling makespan.

## 6 Discussions and Conclusions

This paper presents a multi-objective ARSP formulation to optimize the delays, throughput (i.e., makespan) and emissions in the presence of uncertainties. An improved evolutionary algorithm EMOE with ACTC and OGIS mechanisms is designed to solve the formulated ARSP model. The ACTC mechanism initialize the population considering the acceptable maximum delay, flight turnaround time and Hamming distance. The OGIS mechanism involves four perspectives of preferred level identification, single-level assessment, cross-level assessment and inducing evolution strategy. The computational results suggest that the proposed optimized method has overall advantages in improving the runway scheduling performance over some metaheuristics and the FCFS strategy. And the performance is more pronounced for high-demand scenarios of more than 60 flights, which has the potential to optimize runway scheduling at high density traffic airports.

We also use the ARSP model and EMOE algorithm to make flexible tradeoffs among delays, makespan and emissions under different minimum schedules, instead of using a traditionally integrated objective function with manual weight setting. The delays under the minimum makespan schedule does differ very much from those under the minmum delay schedule. The benefit from minimizing the scheduling makespan comes at the expense of increasing flight delays. Additionally, the delays under the minimum emission schedule also differ from those under the minimum delay schedule. However, the makespan and emissions under the minimum delay schedule can approach the minimum value. The tradeoff analyses suggest that the minimum delay schedule is the best choice to make satisfactory tradeoffs among delays, makespan and emissions in the real practice.

The significance of this paper is an efficient ARSP method with uncertainty considerations, which is featured with a set of Pareto optimal solutions under different traffic management initiatives, such as the minimum delay schedule, the minimum makespan schedule, and the minimum emission schedule. It has the potential to support decision making from multiple perspectives of operation performance. In subsequent work, we will make further efforts to focus on the integrated management of runway configuration and scheduling. Additionally, the runway rescheduling (i.e., retiming and rerouting) problem under disturbed conditions will also be paid close attention in the future work.

**Acknowledgements** This work is supported by the National Natural Science Foundation of China (Grant Nos. 52002178 and 71971112), Natural Science Foundation of Jiangsu Province (Grant No. BK20190416), China Postdoctoral Science Foundation (Grant No. 2017 M611809) and Jiangsu Planned Projects for Postdoctoral Research Funds (Grant No. 1701099C).

## References

Atkin JA, Burke EK, Greenwood JS, Reeson D (2007) Hybrid metaheuristics to aid runway scheduling at London Heathrow airport. Transp Sci 41(1):90–106

Atkin JA, Burke EK, Greenwood JS, Reeson D (2008) On-line decision support for take-off runway scheduling with uncertain taxiing times at London Heathrow airport. J Sched 11(5):323–346

Avella P, Boccia M, Mannino C, Vasilyev I (2017) Time-indexed formulations for the runway scheduling problem. Transp Sci 51(4):1196–1209

Balakrishnan H, Chandran B (2006) Scheduling aircraft landings under constrained position shifting. AIAA Guidance, Navigation, and Control Conference and Exhibit, pp 1–21

Balakrishnan H, Chandran BG (2010) Algorithms for scheduling runway operations under constrained position shifting. Oper Res 58(6):1650–1665

Bayen AM, Tomlin CJ, Ye Y, Zhang J (2004) An approximation algorithm for scheduling aircraft with holding time. 43rd IEEE Conference on Decision and Control, pp 2760–2767

Beasley JE, Sonander J, Havelock P (2001) Scheduling aircraft landings at London Heathrow using a population heuristic. J Oper Res Soc 52(5):83–493

Bennell JA, Mesgarpour M, Potts CN (2011) Airport runway scheduling. 4OR 9(2):115–138

Bennell JA, Mesgarpour M, Potts CN (2017) Dynamic scheduling of aircraft landings. Eur J Oper Res 258(1): 315–327

Bojanowski L, Harikiopoulo D, Neogi N (2011) Multi-runway aircraft sequencing at congested airports. American Control Conference, pp 2752–2758

Bosson C, Xue M, Zelinski S (2015) Optimizing integrated arrival, departure and surface operations under uncertainty. NASA, NASA Technical Reports, pp 1–10

Brentnall AR (2006) Aircraft arrival management. University of Southampton, Doctoral dissertation

D'Ariano A, Pacciarelli D, Pistelli M, Pranzo M (2015) Real-time scheduling of aircraft arrivals and departures in a terminal maneuvering area. Networks 65(3):212–227

Deb K, Pratap A, Agarwal S, Meyarivan TAMT (2002) A fast and elitist multiobjective genetic algorithm: NSGA-II. IEEE Trans Evol Comput 6(2):182–197

Furini F, Kidd MP, Persiani CA, Toth P (2015) Improved rolling horizon approaches to the aircraft sequencing problem. J Sched 18(5):435–447

Gupta G, Malik W, Jung Y (2011) Effect of uncertainty on deterministic runway scheduling. In: 11th AIAA Aviation Technology, Integration, and Operations (ATIO) Conference, pp 1–16

Hamid N, Abounacer R, Idali Oumhand M, Feddaoui MB, Agliz D (2019) Parameters identification of photovoltaic solar cells and module using the genetic algorithm with convex combination crossover. International Journal of Ambient Energy 40(5):517–524

Hansen JV (2004) Genetic search methods in air traffic control. Comput Oper Res 31(3):445–459

Han K, Eve G, Friesz TL (2019) Computing dynamic user equilibria on large-scale networks with software implementation. Netw Spat Econ 19(3):869–902

Heidt A, Helmke H, Liers F, Martin A (2014) Robust runway scheduling using a time-indexed model. 4th SESAR Innovation Days:1–8

Heidt A, Helmke H, Kapolke M, Liers F, Martin A (2016) Robust runway scheduling under uncertain conditions. J Air Transp Manag 56:28–37

Hesselink HH, Paul S (1998) Planning aircraft movements in airports with constraint satisfaction. In: 3rd IMA Conference on Mathematics in Transport Planning and Control:391–400

Hu XB, Di Paolo E (2008) Binary-representation-based genetic algorithm for aircraft arrival sequencing and scheduling. IEEE Trans Intell Transp Syst 9(2):301–310

Kim B, Li L, Clarke JP (2010) Runway assignment by minimizing emissions in terminal airspace. In AIAA Guidance, Navigation, and Control Conference:1–20

Lee H, Balakrishnan H (2008) Fuel cost, delay and throughput tradeoffs in runway scheduling. In American Control Conference:2449–2454

Lieder A, Stolletz R (2016) Scheduling aircraft take-offs and landings on interdependent and heterogeneous runways. Transp Res Part E: Logistics and Transportation Review 88:167–188

Lozano S, Gutiérrez E (2011) Efficiency analysis and target setting of Spanish airports. Netw Spat Econ 11(1): 139–157

Luenberger RA (1988) A traveling-salesman-based approach to aircraft scheduling in the terminal area. NASA, Ames Research Center, Mountain View, pp 1–24

Ma Y, Hu M, Zhang H, Yin J, Wu F (2015) Optimized method for collaborative arrival sequencing and scheduling in metroplex terminal area. Acta Aeronautica et Astronautica Sinica 36(7):2279–2290

Ma Y, Hu M, Yin J, Tian W (2017) Collaborative sequencing and scheduling method for arrival and departure traffic flow in multi-airport terminal area. Acta Aeronautica et Astronautica Sinica 38(2):320222

Malik W, Lee H, Jung YC (2016) Runway scheduling for Charlotte Douglas International airport. The 16th AIAA Aviation Technology, Integration, and Operations Conference, pp 1–11

Martyna J (2012) Runway scheduling with holding pattern and service priority. Automatyka / Automatics 16(2):137–144

Mesgarpour M, Potts CN, Bennell JA (2010) Models for aircraft landing optimization. 4th International Conference on Research in Air Transportation, pp 1–4
Michalewicz, Z. Genetic algorithms + data structures = evolution programs. Springer Science & Business Media, 1996
Montoya J, Rathinam S, Wood Z (2014) Multiobjective departure runway scheduling using dynamic programming. IEEE Trans Intell Transp Syst 15(1):399–413
Ng KKH, Lee CKM, Chan FTS (2017) A robust optimisation approach to the aircraft sequencing and scheduling problem with runway configuration planning. In: 2017 IEEE International Conference on Industrial Engineering and Engineering Management (IEEM), pp 40–44
Ng KKH, Lee CKM, Chan FT, Qin Y (2017a) Robust aircraft sequencing and scheduling problem with arrival/departure delay using the min-max regret approach. Transp. Res. Part E: Logistics and Transportation Review 106:115–136
Ng KKH, Lee CKM, Chan FT, Lv Y (2018) Review on meta-heuristics approaches for airside operation research. Appl Soft Comput 66:104–133
Ng KKH, Lee CK, Chan FT, Chen CH, Qin Y (2020) A two-stage robust optimisation for terminal traffic flow problem. Appl Soft Comput 89:106048
Nikoleris T, Hansen M, Ketcham F (2010) Airport and airspace traffic modeling methods for NextGen. In AIAA Modeling and Simulation Technologies Conference:1–9
Rathinam S, Wood Z, Sridhar B, Jung Y (2009) A generalized dynamic programming approach for a departure scheduling problem. AIAA Guidance, Navigation, and Control Conference, pp 1–12
Sabar NR, Kendall G (2015) An iterated local search with multiple perturbation operators and time varying perturbation strength for the aircraft landing problem. Omega 56:88–98
Samà M, D'Ariano A, Pacciarelli D (2013) Rolling horizon approach for aircraft scheduling in the terminal control area of busy airports. Transp Res Part E: Logistics and Transportation Review 60(1):140–155
Samà M, D'Ariano A, D'Ariano P, Pacciarelli D (2017a) Scheduling models for optimal aircraft traffic control at busy airports: tardiness, priorities, equity and violations consideration. Omega 67(1):81–98
Samà M, D'Ariano A, Corman F, Pacciarelli D (2017b) Metaheuristics for efficient aircraft scheduling and re-routing at busy terminal control areas. Transp. Res. Part C: Emerging Technologies 80:485–511
Samà M, D'Ariano A, Corman F, Pacciarelli D (2018) Coordination of scheduling decisions in the management of airport airspace and taxiway operations. Transp Res Part A: Policy and Practice 114(B):398–411
Smeltink JW, Soomer MJ, de Waal PR, van der Mei RD (2003) Optimisation of airport taxi planning. National Aerospace Laboratory NLR, NLR-TP-2003-475
Sölveling G (2012) Stochastic programming methods for scheduling of airport runway operations under uncertainty. Doctoral dissertation, Georgia Institute of Technology
Sölveling G, Clarke JP (2014) Scheduling of airport runway operations using stochastic branch and bound methods. Transp Res Part C: Emerging Technologies 45:119–137
Sölveling G, Solak S, Clarke JPB, Johnson EL (2011) Scheduling of runway operations for reduced environmental impact. Transp Res Part D: Transport and Environment 16(2):110–120
Vadlamani S, Hosseini S (2014) A novel heuristic approach for solving aircraft landing problem with single runway. J Air Transp Manag 40:144–148
Xue M, Zelinski S (2015) Integrated arrival-and departure-schedule optimization under uncertainty. J Aircr 52(5):1437–1443
Yan S, Hsiao FY, Chen YC (2015) Inter-school bus scheduling under stochastic travel times. Netw Spat Econ 15(4):1049–1074
Yan S, Lu CC, Hsieh JH, Lin HC (2019) A dynamic and flexible berth allocation model with stochastic vessel arrival times. Netw Spat Econ 19(3):903–927
Yin J, Hu M, Peng Y, Tang Y, Ma Y (2014a) Optimized method for multi-runway spatio-temporal resource scheduling in the mode of dependent approaches. Acta Aeronautica et Astronautica Sinica 35(11):3064–3073
Yin J, Hu M, Zhang H, Ma Y (2014b) Optimization approach for collaborative operating modes of multi-runway systems. Acta Aeronautica et Astronautica Sinica 35(3):795–806
Yin J, Hu M, Zhang H, Ma Y, Wu F (2015) Optimized method for multi-runway spatio-temporal resource scheduling in the mode of independent departures. Acta Aeronautica et Astronautica Sinica 36(5):1574–1584
Yin J, Hu M, Ma Y, Han K, Chen D (2019) Airport taxi situation awareness with a macroscopic distribution network analysis. Netw Spat Econ 19(3):669–695

## Affiliations

**Jianan Yin[1,2] · Yuanyuan Ma[3] · Yuxin Hu[3] · Ke Han[4] · Suwan Yin[2] · Hua Xie[1]**

[1] National Key Laboratory of Air Traffic Flow Management, Nanjing University of Aeronautics and Astronautics, Nanjing 211106, China

[2] Department of Civil and Environmental Engineering, Imperial College London, London SW7 2AZ, UK

[3] State Key Laboratory of Air Traffic Management System and Technology, The 28th Research Institute of China Electronics Technology Group Corporation, Nanjing 210007, China

[4] Institute of System Science and Engineering, School of Transportation and Logistics, Southwest Jiaotong University, Chengdu 611756, China

# Terms and Conditions

Springer Nature journal content, brought to you courtesy of Springer Nature Customer Service Center GmbH ("Springer Nature").

Springer Nature supports a reasonable amount of sharing of research papers by authors, subscribers and authorised users ("Users"), for small-scale personal, non-commercial use provided that all copyright, trade and service marks and other proprietary notices are maintained. By accessing, sharing, receiving or otherwise using the Springer Nature journal content you agree to these terms of use ("Terms"). For these purposes, Springer Nature considers academic use (by researchers and students) to be non-commercial.

These Terms are supplementary and will apply in addition to any applicable website terms and conditions, a relevant site licence or a personal subscription. These Terms will prevail over any conflict or ambiguity with regards to the relevant terms, a site licence or a personal subscription (to the extent of the conflict or ambiguity only). For Creative Commons-licensed articles, the terms of the Creative Commons license used will apply.

We collect and use personal data to provide access to the Springer Nature journal content. We may also use these personal data internally within ResearchGate and Springer Nature and as agreed share it, in an anonymised way, for purposes of tracking, analysis and reporting. We will not otherwise disclose your personal data outside the ResearchGate or the Springer Nature group of companies unless we have your permission as detailed in the Privacy Policy.

While Users may use the Springer Nature journal content for small scale, personal non-commercial use, it is important to note that Users may not:

1. use such content for the purpose of providing other users with access on a regular or large scale basis or as a means to circumvent access control;
2. use such content where to do so would be considered a criminal or statutory offence in any jurisdiction, or gives rise to civil liability, or is otherwise unlawful;
3. falsely or misleadingly imply or suggest endorsement, approval , sponsorship, or association unless explicitly agreed to by Springer Nature in writing;
4. use bots or other automated methods to access the content or redirect messages
5. override any security feature or exclusionary protocol; or
6. share the content in order to create substitute for Springer Nature products or services or a systematic database of Springer Nature journal content.

In line with the restriction against commercial use, Springer Nature does not permit the creation of a product or service that creates revenue, royalties, rent or income from our content or its inclusion as part of a paid for service or for other commercial gain. Springer Nature journal content cannot be used for inter-library loans and librarians may not upload Springer Nature journal content on a large scale into their, or any other, institutional repository.

These terms of use are reviewed regularly and may be amended at any time. Springer Nature is not obligated to publish any information or content on this website and may remove it or features or functionality at our sole discretion, at any time with or without notice. Springer Nature may revoke this licence to you at any time and remove access to any copies of the Springer Nature journal content which have been saved.

To the fullest extent permitted by law, Springer Nature makes no warranties, representations or guarantees to Users, either express or implied with respect to the Springer nature journal content and all parties disclaim and waive any implied warranties or warranties imposed by law, including merchantability or fitness for any particular purpose.

Please note that these rights do not automatically extend to content, data or other material published by Springer Nature that may be licensed from third parties.

If you would like to use or distribute our Springer Nature journal content to a wider audience or on a regular basis or in any other manner not expressly permitted by these Terms, please contact Springer Nature at

onlineservice@springernature.com